Annu. Rev. Plant Physiol. Plant Mol. Biol. 2001. 52:817–45

PLANT PLASMA MEMBRANE H^+-ATPases: Powerhouses for Nutrient Uptake

Michael G Palmgren
Department of Plant Biology, The Royal Veterinary and Agricultural University, Thorvaldsensvej 40, DK-1871 Frederiksberg C, Denmark; e-mail: palmgren@biobase.dk

Key Words Arabidopsis, proton pump, genome sequencing, T-DNA knockouts, gene family, 14-3-3, structure

■ **Abstract** Most transport proteins in plant cells are energized by electrochemical gradients of protons across the plasma membrane. The formation of these gradients is due to the action of plasma membrane H^+ pumps fuelled by ATP. The plasma membrane H^+-ATPases share a membrane topography and general mechanism of action with other P-type ATPases, but differ in regulatory properties. Recent advances in the field include the identification of the complete H^+-ATPase gene family in Arabidopsis, analysis of H^+-ATPase function by the methods of reverse genetics, an improved understanding of the posttranslational regulation of pump activity by 14-3-3 proteins, novel insights into the H^+ transport mechanism, and progress in structural biology. Furthermore, the elucidation of the three-dimensional structure of a related Ca^{2+} pump has implications for understanding of structure-function relationships for the plant plasma membrane H^+-ATPase.

CONTENTS

INTRODUCTION

Plasma membrane H^+-ATPases constitute a family of proton pumps driven by hydrolysis of ATP and are found exclusively in the plasma membrane of plants and fungi. Here their primary role is to provide an energy source for transport of nutrients into the cell. The plasma membrane H^+-ATPase is an electrogenic enzyme since it extrudes positive charges (H^+) and thus forms a membrane potential (negative on the inside). In plant cells this membrane potential may exceed −200 mV (52). As protons accumulate on the outside of the cell, the pH of the apoplast decreases typically to reach values of pH 5–6, substantially more acidic than the cytoplasm. The combined electrochemical gradient of charge and matter constitutes a driving force for solutes to enter the cell. Cations are attracted by the cell because of the membrane potential, negative inside, and may enter the cell simply through channel proteins. Cations, anions, and neutral solutes are all able to enter the cell through various carrier proteins through which transport is energized by the concomitant uptake of protons. Thus, most of the hundreds of membrane-bound transport proteins that have been identified in plants are energized indirectly through the action of plasma membrane H^+-ATPases (Figure 1).

In this review, I focus on recent advances that have increased our knowledge of plant plasma membrane H^+-ATPases. These include new insights into the evolution of H^+-ATPases, progress in understanding the physiological roles of H^+-ATPases and their regulation, and advances in structural biology that have helped us to understand structure-function relationships. Other aspects of plasma membrane H^+-ATPases are discussed in a number of recent reviews (79, 82 95, 96, 109, 123, 131, 133).

EVOLUTION

Plasma membrane H^+-ATPase differ markedly from V-type and F-type H^+-ATPases in the vacuolar and mitochondrial inner membranes, respectively, with respect to their biochemistry, subunit organization, mechanism of action and evolutionary origin. Plant plasma membrane H^+-ATPase is a single polypeptide of around 100 kDa that forms a covalent enzyme-phosphate transition state during the reaction cycle (20, 136). Hence, this enzyme is classified as a P-type ATPase (to reflect the presence of the *E*-P form). P-type ATPases constitute a large family

of cation pumps that (*a*) form an aspartyl phosphate reaction cycle intermediate, (*b*) are inhibited by vanadate, and (*c*) share a common domain organization (12, 73, 80, 106). Other ATPases belonging to this family include the fungal plasma membrane H^+-ATPases; the animal Na^+/K^+-ATPase; the gastric H^+/K^+-ATPase; the Ca^{2+}-ATPases in the sarcoplasmic reticulum and in the plasma membrane, vacuolar membrane, and ER of plants, fungi, and animals; heavy metal ATPases in bacteria and eukaryotes; and bacterial K^+-ATPases. In all these ATPases, the amino acid sequence surrounding the phosphorylated aspartate residue is conserved: DKTGT[L/I/V/M][T/I] (the D is phosphorylated). This motif (ProSite PS00154; ATPASE_E1_E2) can be used as a signature pattern to identify P-type ATPases.

P-type ATPases are structurally related to a large superfamily of hydrolases that are typified by the L-2 haloacid dehalogenase (HAD) (8). Sequence and structure comparisons suggest that the catalytic phosphorylation site and other regions are related in P-type ATPases and haloacid dehalogenases (130, 134). However, in P-type ATPases, a nucleotide binding domain has been inserted into the haloacid dehalogenase fold (130, 134). It was therefore hypothesized that P-type ATPases first evolved from the fusion of a HAD-like phophatase with a nucleotide-binding protein (Figure 2). A soluble P-type ATPase was recently identified in the archaebacterium *Methanococcus jannaschii* (91) and might represent an ancestral P-type ATPase.

Later, soluble P-type ATPases might have fused with a membrane-bound carrier protein (Figure 2). The soluble P-type ATPase of *M. jannaschii* has sequence homology with the membrane-bound KdpB-ATPase (91). This primitive bacterial P-type ATPase has only six putative transmembrane segments, whereas present-day plasma membrane H^+-ATPases are believed to have ten transmembrane segments. Acquisition of the four additional membrane-spanning segments might have been the result of subsequent protein fusions.

The KdpB ATPase of eubacteria is unlike other P-type ATPases because it is organized in a complex with three other polypeptides, KdpA, KdpC, and KdpF (2, 42). The Kdp-ATPase complex is involved in K^+ transport but, intriguingly, KdpA, and not KdpB, constitutes the K^+ pathway in the complex (23, 32). It has been suggested (12) that KdpB might be involved in the outward transport of another cation (which could be H^+), thus generating a membrane potential that could drive uptake of K^+ through the KdpA subunit, which resembles a K^+ channel (32); however, experimental evidence for this hypothesis is lacking.

It is not yet clear whether transport of protons by P-type ATPases is to be considered a primitive character. Sequences belonging to the subfamily of P-type H^+-ATPases have been identified in plants, fungi, protozoa, and in *M. jannaschii* (12). However, related genes have not been identified in other archaebacteria (five complete genomes are available so far) and not at all in eubacteria. All bacterial P-type ATPases investigated to date transport divalent cations (heavy metals, Ca^{2+}, and Mg^{2+}) except for the Kdp-ATPase complex.

THE PLASMA MEMBRANE H^+-ATPase GENE FAMILY

The first plant plasma membrane H^+-ATPase genes to be cloned—and the first genes encoding plasma membrane proteins—were Arabidopsis *AHA1* and *AHA3* (49, 101). It soon became apparent that in this organism there is a multigene family encoding H^+-ATPases (47, 48, 54) and, as the Arabidopsis genome sequencing project (17) has reached its completion (133a), we now know that there are 12 Arabidopsis H^+-ATPase genes (Table 1). One of the genes (*AHA12*) carries two large deletions and thus might represent a pseudogene. In the *Nicotiana plumbaginifolia* genome, nine H^+-ATPase genes have been identified (18a, 94), which supports the notion that a large family of plasma membrane H^+-ATPases is present in every plant. References to H^+-ATPase genes in other plants are given in (82) and at the P-type ATPase database web-site (http://biobase.dk/∼axe/Patbase.html).

A phylogenetic tree based on the available amino acid sequences reveals the presence of a number of H^+-ATPase subfamilies (Figure 3). Arabidopsis AHA1,

TABLE 1 Overview of the plasma membrane H^+-ATPase gene family in *Arabidopsis thaliana*

Accession no.	Gene name	Chromosomal location (Centimorgans)[a]	Mol.Wt.[b]	pI	Length (amino acids)
P20649[c]/AC003673[d]	AHA1/At2g18960	2; 35	104313	6.3	949
P19456/AL161576	AHA2/At4g30190	4; 81	104401	6.5	948
P20431/AB019233	AHA3/At5g57350	5; 114	104449	6.7	949
Q9SU58/AL049658	AHA4/At3g47950	3; 65	105679	6.1	960
Q9SJB3/AC006954	AHA5/At2g24520	2; 39	104739	6.8	949
Q9SH76/AC007662	AHA6/At2g07560	2; 19	105012	5.8	949
Q9LY32/AL163852	AHA7/At3g60330	3; 78	105520	6.4	961
Q9M2A0/AL138640	AHA8/At3g42640	3; 53	104131	5.5	948
Q42556/AC011713	AHA9/At1g80660	1; 124	105208	6.0	954
Q43128/S74033[e]	AHA10/At1g17260	1; 23	104815	6.0	947
Q9LV11/AB020751	AHA11/At5g62670	5; 119	105123	6.1	956
Q9T0E0/AL049500[f]	AHA12/At4g11730	4; 40	90439	6.4	813

[a]The position in centimorgans is the position of the nearest known genetic marker according to the Arabidopsis Information Resource (http://www.arabidopsis.org).

[b]Mol. wt., calculated molecular weight.

[c]SWISS-PROT database accession no.

[d]EMBL/GenBank/DDBJ databases accession no.

[e]The original protein sequence is partly derived from genomic DNA data. A proposed exon border has been changed by one amino acid removing a one amino acid gap only found in this sequence.

[f]This sequence is atypical as it is missing 100 amino acid residues from a conserved area and the C-terminal also seems to be missing. In its current form it cannot be an active ATPase, but could be a pseudo-gene or have another function in the cell.

AHA2, AHA3, and AHA5 group together with *N. plumbaginifolia* PMA4. Arabidopsis AHA6, AHA8, and AHA9 belong to a cluster with *N. plumbaginifolia* PMA6. The remaining H^+-ATPases form three small branches, each with representatives from both Arabidopsis and *N. plumbaginifolia*.

When the structures of the Arabidopsis and *N. plumbaginifolia* H^+-ATPase genes are compared and grouped according to their exon split boundaries, the H^+-ATPase genes form three clusters with very similar exon structures (Figure 4). The H^+-ATPases cluster as in the phylogenetic tree, except that one cluster (III) comprises three of the small branches in the phylogenetic tree.

We might conclude that at least two H^+-ATPase gene duplications have occurred early in plant evolution, well before the split between Arabidopsis and *N. plumbaginifolia*. These have been followed by several more recent gene duplications and have given rise to additional subfamilies of H^+-ATPases, each with one or more members depending on the organism.

Is there functional analogy between the H^+-ATPases in each subfamily? For example, Arabidopsis AHA3 and *N. plumbaginifolia* PMA4 are members of the same subfamily (I) and are both localized to the phloem (see below) where they may have the same function. Whether this reflects the general picture, however, is still too early to say.

Another important question is: Do the various members of the H^+-ATPase family in a given species have different catalytic properties? This problem has been tackled by producing individual plant H^+-ATPase isoforms in a heterologous system such as yeast. Subsequent analysis has revealed a number of quantitative differences in catalytic and regulatory properties between isoforms (27a, 72, 97). In yeast, plant H^+-ATPase isoforms are phosphorylated to various degrees by an endogenous protein kinase at residues important for regulation (27a, 39, 76). Are some of the observed differences in catalytic properties between isoforms partly or fully the result of this posttranslational modification in the heterologous host? Identification and disruption of the protein kinase(s) having plant H^+-ATPase as its substrate might help resolve this question.

PHYSIOLOGICAL ROLES

Plasma membrane H^+-ATPases are found throughout the plant in every cell type investigated. However, certain cell types have much higher concentrations of H^+-ATPase than others. For a comprehensive description of the expression pattern of seven isoforms of the *N. plumbaginifolia* plasma membrane H^+-ATPase, the reader is referred to (94). An overview of the localization of plant plasma membrane H^+-ATPases is given in Table 2. In general, cell types with abundant H^+-ATPase are specialized for intensely active transport and accumulate solutes from their surroundings. Although this indicates a role of H^+-ATPases in energizing transport, direct demonstration of the role of H^+-ATPases in the various parts of the plant has to come from genetic studies.

TABLE 2 Localization of specific plasma membrane H^+-ATPase isoforms in the plant body

Tissue	H^+-ATPase protein	Plant	References
Seedlings			
Cotyledon	PMA1, PMA2, PMA4	*N. plumbaginifolia*	79a, 81
Primary root	PMA1, PMA4	*N. plumbaginifolia*	79a, 81
Root:			
Cortex parenchyma	PMA2, PMA3, PMA4	*N. plumbaginifolia*	1
Extension zone	PMA4	*N. plumbaginifolia*	81
Lateral root initials	PMA2, PMA4	*N. plumbaginifolia*	81
Lateral roots	PMA4, PMA9	*N. plumbaginifolia*	81, 94
Root hair and epidermis	PMA1, PMA3, PMA4	*N. plumbaginifolia*	79a, 81
	MHA2	*Zea mays*	36a
Root cap	PMA2, PMA4	*N. plumbaginifolia*	81
Stele (central cylinder)	PMA2, PMA3, PMA4	*N. plumbaginifolia*	81
Uninfected host cells in root nodules	BHA1	*Phaseolus vulgaris*	24a
Stem:			
Axillary buds	PMA2, PMA4, PMA9	*N. plumbaginifolia*	81, 94
Cortex parenchyma	PMA1, PMA2, PMA4	*N. plumbaginifolia*	79a, 81
Pith	PMA4	*N. plumbaginifolia*	81
Vascular tissue	PMA2, PMA3, PMA4, PMA9	*N. plumbaginifolia*	81, 94
	MHA2	*Zea mays*	36a
	AHA3	*A. thaliana*	30, 31
Leaf:			
Guard cells	PMA2, PMA4	*N. plumbaginifolia*	79a, 81
	VHA1, VHA2	*Vicia faba*	51
	MHA2	*Zea mays*	36a
Mesophyll	PMA2, PMA4	*N. plumbaginifolia*	81
	VHA1, VHA2	*Vicia faba*	51
Trichomes (long)	PMA4	*N. plumbaginifolia*	81
Trichomes (short)	PMA6	*N. plumbaginifolia*	94
Vascular tissue	PMA2, PMA3, PMA4	*N. plumbaginifolia*	81
	MHA2	*Zea mays*	36a
	AHA3	*A. thaliana*	30, 31

(*Continued*)

TABLE 2 (*Continued*)

Tissue	H+-ATPase protein	Plant	References
Flower			
Carpel	PMA2	*N. plumbaginifolia*	81
Ovules	PMA1, PMA2, PMA3, PMA4, PMA6, PMA9	*N. plumbaginifolia*	79a, 81, 94
	AH3	*A. thaliana*	30
	AHA10	*A. thaliana*	48
Nectaries	PMA2	*N. plumbaginifolia*	81
Stamen (filament, anther); pollen (grains, tubes)	PMA1, PMA2, PMA3, PMA4, PMA6, PMA9	*N. plumbaginifolia*	79a, 81, 94
	AHA3	*A. thaliana*	30
	AHA9	*A. thaliana*	54
Style	PMA1, PMA3, PMA4	*N. plumbaginifolia*	79a, 81
Vascular tissue	PMA1, PMA2, PMA3, PMA4, PMA6	*N. plumbaginifolia*	79a, 81, 94
	AHA3	*A. thaliana*	30

Massive screening of Arabidopsis lines carrying T-DNA insertions has so far resulted in the identification of individual mutant lines carrying knockouts in all H+-ATPase genes except for AHA6 and AHA12 (66, 67, 149a). Several mutant alleles have been identified for a number of isoforms (149a). The analysis of knockout lines is likely to concentrate first on the identification of essential genes. In those cases where there is redundancy of gene function, single gene mutations might not result in a visible phenotype. However, knockouts in more than a single H+-ATPase gene can in principle be generated by crossing mutant lines.

In this review, focus is on the role of H+-ATPase in phloem loading, the movements of stomatal guard cells, energization of nutrient uptake into the roots, and for the growth of root hairs and pollen tubes. The participation of plasma membrane H+-ATPases in other important physiological processes such as salt and osmotolerance, leaf movements, intracellular pH regulation, and acid growth is discussed elsewhere (79, 82, 94, 96, 123, 131).

Role in Phloem Loading

The plasma membrane H+-ATPase is highly concentrated in the phloem, a specialized tissue for long-distance transport of mostly organic compounds. This was first shown by immunodecoration of this tissue with anti-H+-ATPase antibodies (103, 139). The expression patterns of the *GUS* reporter gene fused to the promoter region of Arabidopsis *AHA3* (29), and *N. plumbaginifolia PMA4* (81) indicate that these H+-ATPase isoforms are phloem localized.

Transgenic *N. plumbaginifolia* plants that cosuppress *PMA4* are stunted in growth and accumulate sugars in the leaves (152). The retarded growth might

result from the inability of established leaves to export sugars to sink organs such as the root and developing leaves. This would suggest that the plasma membrane H^+-ATPase is crucial for the loading of sucrose and probably other photosynthetic assimilates into the phloem (152).

The exact localization of H^+-ATPase in the phloem has been studied in some detail. Arabidopsis AHA3 H^+-ATPase was equipped with a viral epitope and expressed in transgenic plants (31). Immunological detection localized the tagged protein to phloem companion cells. These cells are rich in mitochondria and hence are able to synthesize the large amounts of ATP required by the H^+-ATPase. In Arabidopsis (129, 135) and *Plantago major* (128), sucrose/H^+ cotransporters are found in the plasma membrane of phloem companion cells. Sucrose taken up by these cells is subsequently transported into the sieve elements by passive diffusion through plasmodesmata.

Surprisingly, sucrose/H^+ cotransporters in tobacco, potato, and tomato are localized exclusively in the plasma membrane of enucleate sieve elements (68). These cells contains few mitochondria, and the H^+-ATPase has not been localized to this cell type. How the H^+-ATPase in the companion cells is able to energize sucrose transport by sucrose/H^+ cotransporters in the sieve elements is not understood. Whether H^+-ATPase has escaped detection in enucleate sieve elements needs to be investigated.

Role in Regulation of the Size of the Stomatal Aperture

When guard cells take up solutes and water, the cells swell and the stomatal aperture widens, allowing CO_2 to enter the leaves through the stomatal pore and to be utilized for photosynthesis. Immunological methods have shown that the plasma membrane H^+-ATPase is enriched in guard cells (16, 139). Two H^+-ATPase genes of *Vicia faba* (*VHA1* and *VHA2*), two H^+-ATPases of *N. plumbaginifolia* (*PMA2* and *PMA4*), and maize *MHA2* are expressed in guard cells. In addition, *V. faba*, *N. plumbaginifolia*, and maize express these genes in many other cell types (Table 2).

Transgenic *N. plumbaginifolia* plants that cosuppress expression of *PMA4* have closed stomatal apertures (152). This is true even in the presence of the fungal phytotoxin fusicoccin, which normally induces strong irreversible activation of H^+-ATPases. The H^+-ATPase is thus likely to be required for the opening process.

Opening and closure of the stomatal aperture are controlled by many factors (9, 150). For example, a short pulse of blue light is sufficient to initiate the opening process. Blue light is presumably registered by a light receptor in the guard cells and the signal transmitted to the guard cell plasma membrane H^+-ATPase. In *V. faba*, this activation occurs less than a minute after the light signal is received, thus activating electrogenic H^+ pumping (5, 10, 63, 116, 122). The complete signal transduction pathway from the blue light receptor to the H^+-ATPase has not been

identified, but involves a protein kinase that by phosphorylation of the H^+-ATPase creates a binding site for regulatory 14-3-3 protein (see below) (63).

Role in Solute Uptake in the Roots

Epidermal cells of plant roots have a very high affinity for anti-H^+-ATPase antibody (55, 119). Several candidate H^+-ATPases have emerged that might be involved in energization of the uptake of nutrients from the soil into the roots. Since they are localized to root epidermal cells and root hairs (Table 2). In Arabidopsis, the mRNA of *AHA2* accumulates in the roots (47), and evidence based on the analysis of the expression patterns of promoter-*GUS* fusions in Arabidopsis have suggested that AHA2 is localized in the root epidermis as well as in other parts of the plant (JF Harper, personal communication; K Drumm & MG Palmgren, unpublished results).

In roots, apart from the epidermal cells, high amounts of immunodetectable H^+-ATPase are apparent in the endodermis (55, 103). The localization of H^+-ATPase in root endodermal tissues suggests a role for the pump in the active loading of solutes into the xylem (103). In Arabidopsis, AHA4 is expressed most strongly in the root endodermis, but also in flowers, as suggested by promoter/*GUS* reporter assays (JF Harper, personal communication).

Role in Tip Growing Systems

Tip-growing systems are single-cell systems that expand in one direction only. Prominent examples of plant tip-growing systems are pollen tubes and root hairs (Figure 5).

High amounts of plasma membrane H^+-ATPase have been localized immunologically to pollen grains, but only low amounts to pollen tubes (87). Large numbers of H^+-ATPase isoforms have been localized by *GUS*-promoter fusion analysis to pollen grains (Table 2).

Using a self-referencing (vibrating) electrode, electric fields can be detected around germinating lily pollen (147). Measurements by proton-selective vibrating microelectrodes have revealed that these currents are generated by fluxes of protons (35). Two closed loops of proton fluxes are present in a long ($\sim$800 μM) pollen tube: The first circuit is around the grain, with protons leaving the pollen grain and entering the pollen tube at its basal end, immediately after the pore; the second proton circuit is localized to the growing tip, with protons leaving the tube below the tip and entering the tube at the extreme apex. The first proton circuit, at the base of the pollen tube, is compatible with the high level of plasma membrane H^+-ATPase at the corresponding position (87). However, the second proton circuit, at the tip of the pollen tube, is not compatible with the apparent lack of H^+-ATPase at this location (87). Further studies are therefore required to clarify the localization of H^+-ATPase in pollen tubes.

The pattern of cytoplasmic pH in the growing pollen tube correlates well with the localization of proton fluxes. Cytosolic pH has been measured in the growing

pollen tube using a wide-field imaging system that allows visualization at low concentrations (less than 1 μM) of the pH-sensitive fluorescent probe 2′,7′-bis-(2-carboxyethyl)-5-(and-6)-carboxyfluorescein (BCECF) (35). Higher concentrations of the indicator dye are often used (37, 77, 104), but apparently dissipate local pH gradients (35). The tip of the growing pollen tube possesses a distinct pH gradient (Figure 5). Thus, the cytoplasm of the extreme apex is slightly acidic (pH $\sim$ 6.8), with an alkaline region (pH up to 7.8) observed immediately below (35). The cytoplasmic pH at the position of the alkaline band oscillates with time, and a clear correlation exists between alkalinization and increased rates of pollen tube growth (35).

Root hairs of barley contain high amounts of immunodetectable plasma membrane H^+-ATPase (119), and several isoforms localize to this structure in other species (see above). Proton-selective vibrating electrodes have also revealed a proton circuit in root hairs (58, 146): Protons enter the root hair at the extreme tip and leave the hair just below the tip (58) (Figure 5). This pattern of proton influx and efflux closely resembles that detected in the pollen tube. However, it is still not known whether proton fluxes in the root hair correlate with changes in cytoplasmic pH and spatial localization of the plasma membrane H^+-ATPase.

Confocal ratio imaging of root hairs has been used to reveal the pH of the cell wall and in the cytoplasm. Root hair initiation in Arabidopsis is associated with a slight alkalinization of the cytoplasm (from approximately pH 7.3 pH up to pH 7.7) and a local wall acidification (from pH 6 down to pH 4.5) at the site of initiation (18). The initiation process is reversibly stopped by adding buffers to raise extracellular pH. These localized changes in pH at the initiation site could be due to changes in plasma membrane H^+-ATPase activity; this proposition should be tested, possibly by a genetic approach.

REGULATION

The C-terminal end of the plasma membrane H^+-ATPase (the C-terminal regulatory domain, hence the R-domain) serves a role as an autoinhibitory regulatory domain. This was demonstrated initially from studies showing that a C-terminal fragment of the H^+-ATPase could be removed by proteases resulting in increased H^+-ATPase activity (98, 99). It was hypothesized that a posttranslational modification in vivo might displace the R-domain, which would lead to pump activation and an enzyme with high affinity for its ligands (95). According to this model, physiological factors that increase H^+-ATPase activity are likely to have this domain as their ultimate target.

Several lines of evidence have suggested a molecular mechanism involving the R-domain that leads to activation of the plasma membrane H^+-ATPase (Figure 6). This model involves 14-3-3 protein, which are regulatory proteins that bind to a large number of target proteins in eukaryotic systems (25, 36, 38). Typically,

14-3-3 proteins will only bind if a Ser (85, 149) or a Thr (39, 76, 132) is phosphorylated in the 14-3-3 binding site of the target. A family of twelve 14-3-3 proteins is found in Arabidopsis and the isoforms have somewhat different affinities for a given target within the cell (116a).

Several lines of evidence led to the identification of 14-3-3 proteins as candidate regulatory proteins of H^+-ATPases: (*a*) 14-3-3 proteins copurified with the binding activity of fusicoccin, a fungal toxin that activates the H^+-ATPase (64, 75, 88); (*b*) proteolytic studies showed that fusicoccin activates plasma membrane H^+-ATPase by a mechanism involving the R-domain (57, 69, 92, 111); and (*c*) there was a strict correlation between the amount of fusicoccin bound to the plasma membrane and the activation of the plasma membrane H^+-ATPase, as would be expected if the fusicoccin receptor interacts directly with the H^+-ATPase (28).

Later it was shown that 14-3-3 protein interacts directly with the R-domain (40, 56, 90). Phosphorylation of the penultimate Thr in the R-domain (Thr948, Thr947, and Thr955 in spinach H^+-ATPase, Arabidopsis AHA2, and *N. plumbaginifolia* PMA2, respectively) results in the formation of the binding site for 14-3-3 protein (39, 76, 132). Binding of 14-3-3 protein to the R-domain is stabilized by the addition of fusicoccin. Interestingly, the fusicoccin binding site is generated only following interaction of the 14-3-3 protein with the R-domain (14, 89, 108). Fusicoccin causes the dissociation rate to diminish, resulting in the formation of an almost irreversible complex (39). Fusicoccin can induce binding of 14-3-3 protein to the R-domain even in the absence of a phosphothreonine at the penultimate position, but the binding is less tight.

Plant plasma membrane H^+-ATPase is phosphorylated at several positions in vivo. A phosphotreonine residue has been identified in purified spinach H^+-ATPase at the penultimate position of the R-domain and is protected from dephosphorylation by 14-3-3 protein (93). Blue light activation of the mung bean H^+-ATPase involves protein kinase–mediated phosphorylation of the pump (63). This phosphorylation involves Ser and Thr residues at the R-domain and is concomitant with binding of 14-3-3 protein. Oat root plasma membrane H^+-ATPase is likewise phosphorylated at both Ser and Thr residues (120) but whether this results in the formation of 14-3-3 binding site(s) is not known.

Binding of 14-3-3 protein to the R-domain results in activation of H^+-ATPase activity (14, 76, 132). To reverse the activation, which is induced by the protein kinase-mediated generation of the 14-3-3 binding site, the R-domain would need to be dephosphorylated by a protein phosphatase (Figure 6). A protein phosphatase 2A activity that could serve such a role has been purified from maize membranes (24).

Intriguingly, it has been reported that plasma membrane H^+-ATPases in some systems is inhibited by phosphorylation and activated by dephosphorylation (29, 71, 138, 148), which is in contrast to the results reported above. In beet root, inhibitory phosphorylation of H^+-ATPase is Ca^{2+} dependent (71). The residue(s) in the H^+-ATPase involved in this negative regulation have not been identified but might be apart from the R-domain (29).

Other factors contribute to posttranslational regulation of H^+-ATPase activity. Lysophospholipids and free fatty acids activate H^+-ATPase activity (100, 105) by a mechanism involving the R-domain (57, 99, 112). Lysophospholipids and free fatty acids are generated when phospholipids are hydrolyzed by a reaction catalyzed by phospholipase A_2. This enzyme, which has been proposed to serve an important role in regulation of the H^+-ATPase in vivo (95, 100, 121) was first identified in oat roots (100) and has been purified from leaves of *Vicia faba* (61, 62).

Other aspects of regulation of the activity of H^+-ATPase are discussed in recent reviews (82, 95, 96, 109). Regulation of the amount of H^+-ATPase in the plant occurs at several levels. Transcriptional and translational levels of regulation have been described elsewhere (82). In addition, controlling the amount of H^+-ATPase by exocytosis and protein turnover has been suggested as a regulatory mechanism (46).

ENZYMOLOGY

P-type ATPases are believed to alternate between at least two major conformations, E_1 and E_2. The E_1 form has high affinity for ATP as well as the ion to be transported out of the cytoplasm. The E_2 form has low affinity for both ligands, but has high affinity for the inhibitor vanadate. Transport of a bound cation from one side of the membrane to the other is associated with the conformational change between E_1 and E_2 (Figure 7). According to the Post-Albers scheme (1, 110), the cation enters from the cytoplasmic side and is bound to the enzyme in the E_1 conformation. Phosphorylation of the invariant aspartyl residue results in the E_1P form of the enzyme, which is then converted to E_2P. The cation, now bound with lower affinity to the same site as before, is then released on the other side of the membrane. Phosphate is released by hydrolysis of the aspartyl phosphate bond, and the E_2 form of the enzyme reverts to E_1. According to this model, the pump operates much like the lock of a waterway, which also has an enclosed section with alternating accessibility to either side.

Protons are ligands of the H^+-ATPase, and therefore pH is expected to strongly influence pump activity. Indeed, kinetic data suggest that protonation on an ionizable group in the AHA2 H^+-ATPase with a pK of $\sim$6.7 stabilizes the high-affinity conformation (E_1) of the enzyme (112).

Similarly, in the Na^+/K^+-ATPase and muscle sarcoplasmic reticulum Ca^{2+}-ATPase, the cations to be bound from the cytoplasmic side (Na^+ and Ca^{2+}, respectively) stabilize the enzyme in the E_1 conformation (59).

When plant plasma membrane H^+-ATPase is activated by mechanisms involving the R-domain, the ATP affinity increases and pH optimum of the pump is displaced towards neutral values, which might reflect an increased H^+ affinity (98, 99, 112). In line with the discussion above, this would suggest that in the activated state the conformational equilibrium of the enzyme has been shifted toward the E_1 form.

STRUCTURE-FUNCTION RELATIONSHIPS

Quaternary Structure

The quaternary structure of the red beet plasma membrane H^+-ATPase has been studied by radiation inactivation experiments. This analysis revealed a H^+-ATPase target size of about 225 kDa in plasma membrane vesicles and 218 kDa in reconstituted liposomes, corresponding to a dimeric form of the enzyme (21). The H^+-ATPase solubilized with the detergent Zwittergent 3-14 enzyme has a target size of 129 kDa, corresponding to the expected mass of a monomer (21). Because the solubilized enzyme is still active, the minimal functional unit of the H^+-ATPase is likely to be a monomer (21). In line with these results, it has been demonstrated that reconstituted monomers of *N. crassa* H^+-ATPase are active proton pumps (43).

Tertiary Structure

Information on the three-dimensional structure of a membrane protein can be obtained from analysis of well-ordered crystals of the purified protein in either two or three dimensions. Only very recently has it been possible to crystallize purified recombinant plant plasma membrane H^+-ATPase for this purpose (T Jahn, J Dietrich, B Andersen, C Otter, C Briving, MG Palmgren, submitted). These crystals of AHA2 diffract to 8 Å resolution, but so far the crystals have been studied only in one plane. The crystal unit cell suggests that the H^+-ATPase is organized in the membrane as a dimer. Furthermore, the cytoplasmic portion of the molecule appears to be divided into three distinct densities, which could correspond to distinct domains of the enzyme.

The plasma membrane H^+-ATPase of the fungus *Neurospora crassa* has been crystallized in two dimensions (11). From analysis of the crystals by cryoelectron microscopy, a structure resolved to 8 Å resolution was obtained. The H^+-ATPase forms hexamers, and ten transmembrane helices are apparent in the crystal structure of each H^+-ATPase molecule. The pump is exposed to both sides of the membrane; however, most of the H^+-ATPase (around 70%) is exposed to one side of the membrane, presumably the cytoplasmic side, and is separated into four more-or-less separated domains.

The recent solution of the crystal structure of the sarcoplasmic reticulum Ca^{2+}-ATPase to 2.6 Å resolution (134) is a landmark in our understanding of structure/function relationships in cation pumps. Since this is the only structure of a P-type ATPase solved at atomic resolution, it serves as a model for the structure of related pumps such as the plasma membrane H^+-ATPase.

In the structure of the Ca^{2+}-ATPase (134), a large cytoplasmic protrusion is associated with a bundle of ten membrane spanning alpha-helices, as in the *Neurospora* H^+-ATPase (11). Although the borders of the membrane are not clearly defined in the structure, some of the transmembrane helices are very long and protrude into the cytoplasmic region of the pump. Very little of the protein mass

is exposed to the extracytoplasmic side. The cytoplasmic region is divided into three well-separated domains: A, P, and N (Figure 8). The actuator domain (A) includes the N-terminal region and the portion of the molecule formed by the small cytosolic loop between M2 and M3. The phosphorylation (P) domain is bounded by M4 and M5 and includes the aspartyl residue to be phosphorylated during catalysis. The nucleotide (N) binding domain is fused to the P-domain and contains the ATP binding site. Thus, the domain structure of the Ca^{2+}-ATPase corresponds very well to the domain organization suggested above in the discussion on the evolution of P-type ATPases.

The primary structure of the Arabidopsis plasma membrane H^+-ATPase AHA2 is indicated in Figure 9. The various domains of the enzyme, as revealed from sequence comparison with the Ca^{2+}-pump, are indicated in colors. The sequence analysis method of von Heijne (143) predicts all ten transmembrane segments in SERCA1 correctly, and similarly predicts ten transmembrane helices in the AHA2 H^+-ATPase (96).

H^+-Binding Site(s)

A 1:1 stoichiometric relationship between ATP being hydrolysed and protons being transported is supported by measurements under a number of experimental conditions (19, 22, 125). However, this does not preclude the possibility that other ratios are possible under other conditions (15, 84) or that one or more protons could be counter-transported by the H^+-ATPase. Thus, hydrolysis of ATP might e.g. result in two protons pumped out and one pumped in (Figure 10). Other P-type ATPases are involved in counter-transport of cations, and in the case of the Ca^{2+}-ATPase, the counterions are indeed protons. Binding of counterions in a number of P-type ATPases appears to be required for hydrolysis of the E_2P phosphoenzyme (80).

By comparison with other ion pumps, at least two models for ion binding can be envisioned. According to the first model, protons will follow a pathway of different polar groups during transport through the membrane (19a). Such a proton-wire mechanism appears to be true for well-characterized H^+ pumps such as bacteriorhodopsin (50, 67a) and cytochrome c oxidase (78, 127). According to the second model, the ion to be transported binds to a specific pocket surrounded by coordinating groups (19a). This model appears to be valid for related P-type ATPases, such as the Ca^{2+}- and Na^+/K^+-ATPase. Assuming a similar transport mechanism in the H^+-ATPase, this raises the question as to whether H^+ is transported as H_3O^+ (18b, 19a), which has about the same ionic radius and Na^+ and Ca^{2+} (Table 3). The observation that heavy water (D_2O) inhibits plasma membrane H^+-ATPase activity in isolated plasma membrane vesicles (118) supports a model that involves translocation of water.

Site-directed mutagenesis and preferably structural studies are required to test which residues are involved in binding of protons by the H^+-ATPase. It has been proposed (134) that binding of Ca^{2+} to the Ca^{2+}-ATPase requires step-wise dehydration of Ca^{2+}, whereas dissociation is associated with rehydration of the bound

TABLE 3 Ionic radii of selected dehydrated cations

Ion	Crystal radii (Å)
H_3O^+	1.15
Na^+	1.12
K^+	1.44
Ca^{2+}	1.06

Ca^{2+}. A similar mechanism might be valid for H^+-ATPases as a hydrated H_3O^+ ion binds three to four water molecules (Figure 11). Likewise, specific binding of a transported H_3O^+ is not likely to involve more than three to four liganding groups per bound H_3O^+ as hydrogen bonding partners. It has been suggested that negatively charged or polar residues in the transmembrane region of H^+-ATPases could be involved in H^+ binding (145). When H^+-ATPase sequences are compared in their presumed transmembrane regions, just one acidic residue is strictly conserved, namely Asp684 (AHA2 numbering) in M6, and among the polar residues only two are conserved (Gln760 and Ser762; both in the middle of M8) (Figure 12).

In the Arabidopsis H^+-ATPase AHA2, Asp684 has been replaced by Asn (22a). This conservative substitution has no effect on folding of the enzyme but completely abolishes proton pumping by the ATPase. The mutagenized enzyme is able to proceed to E_1 P but from here it appears to be blocked in its catalytic cycle. Thus, these data are compatible with Asp684 being involved in coordination of H^+. In the yeast H^+-ATPase PMA1, many residues in transmembrane regions have been individually mutated (4, 33, 45, 124), including Asp730 (45; in M6), which corresponds to AHA2 Asp684. However, in the yeast enzyme, Asp730 cannot be substituted alone since this residue is apparently involved in forming a salt bridge with Arg695 in M5, and in its absence, PMA1 does not fold properly (45).

In the calcium pump structure, two calcium ions are bound side by side in the same plane as the membrane (134). Site I is located between M5 and M6, whereas site II is between M4 and M6) (Figure 13). In site II, three carbonyl groups of hydrophobic amino acid residues contribute to coordination of the bound Ca^{2+} (Figure 14). Carbonyl groups are normally hidden in the core of alpha-helices, but two prolines separated by three residues partially unfold the alpha-helical structure of M4 and allow the coordinating carbonyl groups to get into close proximity to Ca^{2+}. In M6, Asp800 (corresponding to AHA2 Asp684) plays a key role as it is coordinating both of the two Ca^{2+} ions bound and is in close proximity to the unwound part of M4 (Figure 15).

A three-dimensional model of the first six transmembrane segments of AHA2 has been built from the coordinates of the Ca^{2+}-pump structure by homology modeling (J Bukrinsky, MJ Buch-Pedersen, S Larsen, MG Palmgren, submitted)

(Figure 13). The details of this model are only suggestions, but it might serve as a useful tool to predict the roles of various residues and domains of the plant H^+-ATPase. In the model of the AHA2 H^+-ATPase, there appears to be no analogy to site I in the SERCA1 Ca^{2+}-ATPase, since the binding pocket apparently is occupied by the side chain of a basic residue, Arg655 (Figure 14). On the other hand, the two proline residues in M4 are strictly conserved between Ca^{2+}- and H^+-ATPases. Accordingly, in the model of the AHA2 H^+-ATPase, M4 is also unfolded (Figure 15) and the position of carbonyl groups in this region would easily allow for coordination of a bound H_3O^+ (Figure 14). Thus, four residues in the transmembrane region of plant plasma membrane H^+-ATPase emerge as candidate coordinating residues in a H_3O^+ binding site: Asp684 in M6 could contribute with its side chain whereas three residues in M4 (Ile282, Gly283, and Ile285) each might contribute with carbonyls (Figure 14). At this location, the H^+ might be shared between the bound water molecule and the carboxyl group of Asp684. In yeast PMA1, the corresponding residues in M4 (Ile331, Ile332, and Val334) have been substituted individually with Ala. These mutants have reduced (around 30%) H^+-ATPase activity but are still able to pump protons (4).

ATP Binding Site

Fluorescein isothiocyanate inhibits activity of the *N. crassa* PMA1 H^+-ATPase by reacting with Lys474 (which in AHA2 corresponds to Lys423) in the well-conserved sequence motif KGAP. Since ATP protects Lys474 from fluorescein isothiocyanate, it was suggested that this residue is located at the nucleotide-binding domain (102). Indeed, in the Ca^{2+}-ATPase structure, the corresponding residue is positioned at the bottom of the predicted ATP binding site formed by the N-domain (134). As noted by Toyoshima and coworkers (134), the ATP binding site in the crystal structure is far (about 25 Å distance) from the aspartyl residue that is phosphorylated by the gamma-phosphoryl group of the bound ATP. This could imply that a substantial conformational change takes place between binding of ATP and formation of the phosphoenzyme.

Mg^{2+} Binding Site

Mg^{2+} is absolutely required by the plasma membrane H^+-ATPase for ATP hydrolysis (136). Modeling the active site of P-type ATPases on the dehalogenase fold (114) has suggested that the Mg^{2+} ion is coordinated by two aspartate residues that in AHA2 H^+-ATPase would correspond to Asp588 and Asp592 (Figure 16) that are part of the segment ^{587}GDGVNDAPALKKA, which is highly conserved among P-type ATPases (12). The bound Mg^{2+} is proposed to be in close proximity to residues that correspond to AHA2 Asp329, the aspartyl residue in the P-domain that gets phosphorylated during catalysis. Mutagenesis studies with the Na^+/K^+-ATPase support the notion that at least Asp710 in Na^+/K^+-ATPase (corresponding to AHA2 Asp588) contribute to Mg^{2+} binding during transfer of the gamma-phosphate of ATP to the aspartyl residue (106a). The role of the bound

Mg^{2+} might be to neutralize the negatively charged phosphate group and, in addition, it could be involved in activation of the attacking neutrophile, polarization of the P–O bond, and stabilization of the leaving group (114).

Catalytic Mechanism

Koonin and coworkers (8) have suggested a reaction scheme for P-type ATPases based on the structural homology between these pumps and haloacid dehalogenases. The reaction scheme of haloacid dehalogenases is known in considerable detail (53, 70, 115). Modified for the plant plasma membrane H^+-ATPase, the following reaction scheme can be proposed (Figure 16): First, Asp329 forms a transition state complex with the gamma-phosphoryl group of ATP. In this complex, one of the excessive negative charges is stabilized by the positive charge of a nearby basic residue, Lys569, and the other charge is balanced by Mg^{2+} (see above). This leads to formation of the aspartyl phosphate pump intermediate. Mg^{2+} would leave again together with ADP. A water molecule is then consumed for hydrolysis of the acylphosphate bond and phosphate is released. It has been proposed that the A domain is involved in catalyzing this phosphatase reaction (123).

Position of the R-domain and Its Intramolecular Receptor

The R-domain of the plant plasma membrane H^+-ATPase comprises approximately 110 residues (Figure 8). Substitutions at several residues in the R-domain of the *N. plumbanifolia* PMA2 result in activated H^+-ATPases in which the R-domain is more vulnerable to proteolytic attack compared to that of the wild-type enzyme (83, 84). Since the substitutions mimic the effect of proteolytic removal of the R-domain, it is plausible that they result in displacement of this domain from the rest of the molecule (83, 84). A mutational study of AHA2 through 87 consecutive residues in the C-terminal domain has revealed that single amino acid substitutions at 23 positions lead to increased pump activity (13). The amino acid substitutions resulting in this phenotype cluster in two groups, regions I and II (Figure 8), that together are likely to form the autoinhibitory region of the R-domain.

The R-domain is likely to interact with a portion of the pump molecule and in this way to exert its negative effect on enzyme activity. Genetic strategies have been employed to identify this intramolecular receptor for the R-domain. Yeast strains containing no endogenous H^+-ATPase activity have been allowed to express plant H^+-ATPase and spontaneous mutations in the plant gene that result in an up-regulated H^+-ATPase could be isolated because they increase the growth rate of the transformed yeast cells. Many of the mutations obtained in this way cluster in regions I and II of the R-domain (15, 83, 84) but, in addition, large numbers of mutations have been observed in other regions of the pump molecule. Thus, in the *N. plumbaginifolia* PMA2 H^+-ATPase polypeptide such mutations are found in the presumed A- and P-domains and in M1 and M4 (83, 84) (Table 4). A similar strategy has been employed to identify regulatory residues in the yeast PMA1 H^+-ATPase (34) and substitutions have been found in essentially the same domains

TABLE 4 Single point mutations in various P-type ATPases that result in activation of pump activity. Mutations identified in R-domains are not indicated

		Corresponding residue in other pumps		
		AHA2	SERCA1	
ATPase	**Mutation**	**#**	**#**	**Domain**
Np-PMA2 (83,84)	E14D,Q,G	E10	K7	A
	P72A	P68	R63	M1 (middle)
	W75C	W71	L66	M1 (middle)
	P154R	P150	P147	A
	V220G	V216	V228	A
	H221N,D	H217	S229	A
	H229D	H225	D237	A-"leg" junction
	P294Q	P290	P312	M4 (top)
	S298L	S294	T316	M4 (top)
	N510K	N506	R620	P
	E626G	E622	D737	P-M5 junction
Sc-PMA1 (34)	A165V	A117	A112	M2 (top)
	V169I/D170N	A121/A122	I116/E117	M2 (top)
	A350T	S301	T323	M4 (top)
	A351T	H302	R324	M4 (top)
	P536L	P489	P603	P-N junction
	A565T	G518	A632	P
	G587N	H541	G655	P
	G648S	G602	G717	P
	P669L	P623	D738	P-M5 junction
	G670S	G624	N739	P-M5 junction
At-ACA2 (27)	E167K	K60	E55	M1 (top)
	D219N	E113	Q108	M2 (top)
	E341K	V233	K246	M3 (top)

but also in M2 (Table 4). Likewise, in the plant Ca^{2+}-ATPase ACA2 (27), which is regulated by an N-terminal regulatory domain, regulatory residues are found in the predicted M1, M2, and M3 (Table 4). The various P-type ATPases regulated by terminal autoinhibitory domains were aligned with the SERCA1 Ca^{2+}-ATPase and the corresponding residues in this pump are indicated in Table 4.

A note of caution is necessary before interpreting these results since "regulatory" mutants might involve the basic machinery involved in conformational transitions rather than specific regulatory properties. Thus, a large number of mutants in both the yeast H^+-ATPase (3) and in the SERCA1 Ca^{2+}-ATPase (7, 26, 41, 113, 140–142, 151) have been identified that are impeded in their ability to undergo the E_1P-E_2P conformational change. In these mutants, the conformational equilibrium is shifted toward the E_1 form, which is characterized by high affinity for ATP. The

mutated residues group in several domains of the ATPases, such as the A- and P-domains, as well as M1, M2, and M4, much like the "regulatory" mutants described above. Ca^{2+}-ATPase E_1P-E_2P conformational change mutants that appear to have the same phenotype behave very differently when the fast kinetics are analyzed in detail by rapid quench experiments (126). Thus, they group into several classes that could involve conformational change mutants, regulatory mutants, etc.

Nevertheless, when residues in the Ca^{2+}-ATPase corresponding to the regulatory substitutions in the various P-type ATPases regulated by terminal autoinhibitory domains are marked in the structure of the Ca^{2+}-pump an interesting picture emerges (Figure 9). The residues affected form an almost continuous line of surface-exposed groups extending from the P-domain to the middle of M1. This raises the question as to whether the R-domain is placed horizontally relative to the rest of the pump molecule in the plane of the membrane, possibly extending into the membrane.

A few lines of evidence support the notion that the R-domain might indeed be close to or partially embedded in the membrane. Thus, (*a*) lysophosphatidylcholine, a lipid molecule, and free fatty acids, that incorporates into membranes, activate plant H^+-ATPase by a mechanism involving the R-domain (see above); (*b*) fusicoccin, which interacts with the R-domain, is a strongly hydrophobic compound and is likely to partition into the membrane; (*c*) a protein kinase identified in spinach that phosphorylates the R-domain of the plasma membrane H^+-ATPase is membrane-associated (132).

CONCLUDING REMARKS

Recent advances in the plasma membrane H^+-ATPase field have allowed links to be made from the level of protein structure and enzyme regulation to cellular function and plant physiology. Important questions that remain to be answered are: What are the cellular and organismal function of all the different H^+-ATPase isoforms? What are the natures of the signal transduction pathways that regulate pump activity? Where are the active sites in H^+-ATPases? What are the structural changes mediating proton translocation? Will it be possible to improve nutrient uptake from the soil by the genetic manipulation of H^+-ATPase crop plants? These and other important questions are already subjected to intense research in several laboratories and exciting new discoveries are expected in the near future.

ACKNOWLEDGMENTS

The author is indebted to Jens Bukrinsky for his work on modeling the AHA2 pump structure, to Kristian B. Axelsen for database searches and construction of phylogenetic trees, to Nina Rasmussen for excellent art work, and to Tom Roberts for editing the manuscript. The work in the author's laboratory was supported by

the European Union's Biotechnology Programme and the Human Frontier Science Program Organization.

LITERATURE CITED

1. Albers RW. 1967. Biochemical aspects of active transport. *Annu. Rev. Biochem.* 36: 727–56
2. Altendorf K, Siebers A, Epstein W. 1992. The KDP ATPase of *Escherichia coli*. *Ann. NY Acad. Sci.* 671:228–43
3. Ambesi A, Miranda M, Petrov VV, Slayman CW. 2000. Biogenesis and function of the yeast plasma-membrane H^+-ATPase. *J. Exp. Biol.* 203:155–60
4. Ambesi A, Pan RL, Slayman CW. 1996. Alanine-scanning mutagenesis along membrane segment 4 of the yeast plasma membrane H^+-ATPase. Effects on structure and function. *J. Biol. Chem.* 271: 22999–3005
5. Amodeo G, Srivastava A, Zeiger E. 1992. Vanadate inhibits blue light-stimulated swelling of *Vicia* guard–cell protoplasts. *Plant Physiol.* 100:1567–70
6. Andersen JP, Vilsen B. 1998. Structure-function relationships of the calcium binding sites of the sarcoplasmic reticulum Ca^{2+}-ATPase. *Acta Physiol. Scand. Suppl.* 643:45–54
7. Andersen JP, Vilsen B, Leberer E, MacLennan DH. 1989. Functional consequences of mutations in the beta-strand sector of the Ca^{2+}-ATPase of sarcoplasmic reticulum. *J. Biol. Chem.* 264:21018–23
8. Aravind L, Galperin MY, Koonin EV. 1998. The catalytic domain of the P-type ATPase has the haloacid dehalogenase fold. *Trends Biochem. Sci.* 23:127–29
9. Assmann SM, Shimazaki K. 1999. The multisensory guard cell. Stomatal responses to blue light and abscisic acid. *Plant Physiol.* 119:809–16
10. Assmann SM, Simoncini L, Schroeder JI. 1985. Blue light activates electrogenic ion pumping in guard cell protoplasts of *Vicia faba* L. *Nature* 318:285–87
11. Auer M, Scarborough GA, Kuhlbrandt W. 1988. Three-dimensional map of the plasma membrane H^+-ATPase in the open conformation. *Nature* 392:840–43
12. Axelsen KB, Palmgren MG. 1998. Evolution of substrate specificities in the P-type ATPase superfamily. *J. Mol. Evol.* 46:84–101
13. Axelsen KB, Venema K, Jahn T, Baunsgaard L, Palmgren MG. 1999. Molecular dissection of the C-terminal regulatory domain of the plant plasma membrane H^+-ATPase AHA2: mapping of residues that when altered give rise to an activated enzyme. *Biochemistry* 38:7227–34
14. Baunsgaard L, Fuglsang AT, Jahn T, Korthout HA, de Boer AH, Palmgren MG. 1998. The 14-3-3 proteins associate with the plant plasma membrane H^+-ATPase to generate a fusicoccin binding complex and a fusicoccin responsive system. *Plant J.* 13:661–71
15. Baunsgaard L, Venema K, Axelsen KB, Villalba JM, Welling A, et al. 1996. Modified plant plasma membrane H^+-ATPase with improved transport coupling efficiency identified by mutant selection in yeast. *Plant J.* 10:451–58
16. Becker D, Zeilinger C, Lohse G, Depta H, Hedrich R. 1993. Identification and biochemical characterization of the plasma membrane H^+-ATPase in guard cells of *Vicia faba* L. *Planta* 190:44–50
17. Bevan M, Bancroft I, Mewes HW, Martienssen R, McCombie R. 1999. Clearing a path through the jungle: progress in Arabidopsis genomics. *BioEssays* 21:110–20
18. Bibikova TN, Jacob T, Dahse I, Gilroy S.

1998. Localized changes in apoplastic and cytoplasmic pH are associated with root hair development in *Arabidopsis thaliana*. *Development* 125:2925–34

18a. Boutry M, Michelet B, Goffeau A. 1989. Molecular cloning of a family of plant genes encoding a protein homologous to plasma membrane H^+-translocating ATPases. *Biochem. Biophys. Res. Commun.* 162:567–74

18b. Boyer PD. 1988. Bioenergetic coupling to protonmotive force: Should we be considering hydronium ion coordination and not group protonation? *Trends Biochem. Sci.* 13:5–7

19. Briskin DP, Basu S, Assmann SM. 1995. Characterization of the red beet plasma membrane H^+-ATPase reconstituted in a planar bilayer system. *Plant Physiol.* 108:393–98

19a. Briskin DP, Hanson JB. 1992. How does the plant plasma membrane H^+-ATPase pump protons? *J. Exp. Bot.* 43:269–89

20. Briskin DP, Poole RJ. 1983. Plasma membrane ATPase of red beet forms a phosphorylated intermediate. *Plant Physiol.* 71:507–12

21. Briskin DP, Reynolds-Niesman I. 1989. Change in target molecular size of the red beet plasma membrane ATPase during solubilization and reconstitution. *Plant Physiol.* 90:394–97

22. Briskin DP, Reynolds-Niesman I. 1991. Determination of H^+/ATP stoichiometry for the plasma membrane H^+-ATPase from red beet (*Beta vulgaris* L.) storage tissue. *Plant Physiol.* 95:242–50

22a. Buch-Pedersen MJ, Venema K, Serrano R, Palmgren MG. 2000. Abolishment of proton pumping and accumulation in the E_1P conformational state of a plant plasma membrane H^+-ATPase by substitution of a conserved aspartyl residue in transmembrane segment 6. *J. Biol. Chem.* 275:39167–73

23. Buurman ET, Kim KT, Epstein W. 1995. Genetic evidence for two sequentially occupied K^+ binding sites in the Kdp transport ATPase. *J. Biol. Chem.* 270: 6678–85

24. Camoni L, Iori V, Marra M, Aducci P. 2000. Phosphorylation-dependent interaction between plant plasma membrane H^+-ATPase and 14-3-3 proteins. *J. Biol. Chem.* 275:9919–23

24a. Campos F, Perez-Castineira JR, Villalba JM, Culianez-Marcia FA, Sanchez F, Serrano R. 1996. Localization of plasma membrane H^+-ATPase in nodules of *Phaseolus vulgaris* L. *Plant Mol. Biol.* 32:1043–53

25. Chung HJ, Sehnke PC, Ferl RJ. 1999. The 14-3-3 proteins: cellular regulators of plant metabolism. *Trends Plant Sci.* 4:367–71

26. Clarke DM, Loo TW, MacLennan DH. 1990. Functional consequences of alterations to polar amino acids located in the transmembrane domain of the Ca^{2+}-ATPase of sarcoplasmic reticulum. *J. Biol. Chem.* 265:6262–67

27. Curran AC, Hwang I, Corbin J, Martinez S, Rayle D, et al. 2000. Autoinhibition of a calmodulin dependent calcium pump involves a structure in the stalk that connects the transmembrane domain to the ATPase catalytic domain. *J. Biol. Chem.* 275:30301–8

27a. Dambly S, Boutry M. 2000. The two major plant plasma membrane H^+-ATPases display different regulatory properties. *J. Biol. Chem.* In press

28. De Michelis MI, Rasi-Caldogno F, Pugliarello MC, Olivari C. 1996. Fusicoccin binding to its plasma membrane receptor and the activation of the plasma membrane H^+-ATPase. 3. Is there a direct interaction between the fusicoccin receptor and the plasma membrane H^+-ATPase? *Plant Physiol.* 110:957–64

29. Desbrosses G, Stelling J, Renaudin JP. 1998. Dephosphorylation activates the purified plant plasma membrane

H^+-ATPase—possible function of phosphothreonine residues in a mechanism not involving the regulatory C-terminal domain of the enzyme. *Eur. J. Biochem.* 251:496–503

30. DeWitt ND, Harper JF, Sussman MR. 1991. Evidence for a plasma membrane proton pump in phloem cells of higher plants. *Plant J.* 1:121–28
31. DeWitt ND, Sussman MR. 1995. Immunocytological localization of an epitope-tagged plasma membrane proton pump (H^+-ATPase) in phloem companion cells. *Plant Cell* 2053–67
32. Durell SR, Bakker EP, Guy HR. 2000. Does the KdpA subunit from the high affinity K^+-translocating P-type KDP-ATPase have a structure similar to that of K^+ channels? *Biophys. J.* 78:188–99
33. Dutra MB, Ambesi A, Slayman CW. 1998. Structure-function relationships in membrane segment 5 of the yeast Pma1 H^+-ATPase. *J. Biol. Chem.* 273:17411–17
34. Eraso P, Portillo F. 1994. Molecular mechanism of regulation of yeast plasma membrane H^+-ATPase by glucose. Interaction between domains and identification of new regulatory sites. *J. Biol. Chem.* 269:10393–99
35. Feijo JA, Sainhas J, Hackett GR, Kunkel JG, Hepler PK. 1999. Growing pollen tubes possess a constitutive alkaline band in the clear zone and a growth-dependent acidic tip. *J. Cell Biol.* 144:483–96
36. Finnie C, Borch J, Collinge DB. 1999. 14-3-3 proteins: eukaryotic regulatory proteins with many functions. *Plant Mol. Biol.* 40:545–54

36a. Frias I, Caldeira MT, Perez-Castineira JR, Navarro-Avino JP, Culianez-Macia FA, et al. 1996. A major isoform of the maize plasma membrane H^+-ATPase: characterization and induction by auxin in coleoptiles. *Plant Cell* 8:1533–44

37. Fricker MD, White NS, Obermeyer G. 1997. pH gradients are not associated with tip growth in pollen tubes of *Lilium longiflorum*. *J. Cell Sci.* 110:1729–40
38. Fu H, Subramanian RR, Masters SC. 2000. 14-3-3 proteins: structure, function, and regulation. *Annu. Rev. Pharmacol. Toxicol.* 40:617–47
39. Fuglsang AT, Visconti S, Drumm K, Jahn T, Stensballe A, et al. 1999. Binding of 14-3-3 protein to the plasma membrane H^+-ATPase AHA2 involves the three C-terminal residues Tyr ^{946}-Thr-Val and requires phosphorylation of Thr^{947}. *J. Biol. Chem.* 274:36774–80
40. Fullone MR, Visconti S, Marra M, Fogliano V, Aducci P. 1998. Fusicoccin effect on the in vitro interaction between plant 14-3-3 proteins and plasma membrane H^+-ATPase. *J. Biol. Chem.* 273:7698–702
41. Garnett C, Sumbilla C, Belda FF, Chen L, Inesi G. 1996. Energy transduction and kinetic regulation by the peptide segment connecting phosphorylation and cation binding domains in transport ATPases. *Biochemistry* 35:11019–25
42. Gassel M, Mollenkamp T, Puppe W, Altendorf K. 1999. The KdpF subunit is part of the K^+-translocating Kdp complex of *Escherichia coli* and is responsible for stabilization of the complex in vitro. *J. Biol. Chem.* 274:37901–7
43. Goormaghtigh E, Chadwick C, Scarborough GA. 1986. Monomers of the *Neurospora* plasma membrane H^+-ATPase catalyze efficient proton translocation. *J. Biol. Chem.* 261:7466–71
44. Guex N, Peitsch MC. 1997. SWISS-MODEL and the Swiss-PdbViewer: an environment for comparative protein modelling. *Electrophoresis* 18:2714–23
45. Gupta SS, DeWitt ND, Allen KE, Slayman CW. 1998. Evidence for a salt bridge between transmembrane segments 5 and 6 of the yeast plasma-membrane H^+-ATPase. *J. Biol. Chem.* 273:34328–34
46. Hager A, Debus G, Edel HG, Stransky H, Serrano R. 1991. Auxin-induced

exocytosis and the rapid synthesis of a high-turnover pool of plasma–membrane H^+-ATPase. *Planta* 185:527–37

47. Harper JF, Manney L, DeWitt ND, Yoo MH, Sussman MR. 1990. The *Arabidopsis thaliana* plasma membrane H^+-ATPase multigene family. Genomic sequence and expression of a third isoform. *J. Biol. Chem.* 265:13601–8
48. Harper JF, Manney L, Sussman MR. 1994. The plasma membrane H^+-ATPase gene family in Arabidopsis: genomic sequence of AHA10 which is expressed primarily in developing seeds. *Mol. Gen. Genet.* 244:572–87
49. Harper JF, Surowy TK, Sussman MR. 1989. Molecular cloning and sequence of cDNA encoding the plasma membrane proton pump (H^+-ATPase) of *Arabidopsis thaliana*. *Proc. Natl. Acad. Sci. USA* 86:1234–38
50. Heberle J. 2000. Proton transfer reactions across bacteriorhodopsin and along the membrane. *Biochim. Biophys. Acta* 1458:135–47
51. Hentzen AE, Smart LB, Wimmers LE, Fang HH, Schroeder JI, Bennett AB. 1996. Two plasma membrane H^+-ATPase genes expressed in guard cells of *Vicia faba* are also expressed throughout the plant. *Plant Cell Physiol.* 37:650–59
52. Hirsch RE, Lewis BD, Spalding EP, Sussman MR. 1998. A role for the AKT1 potassium channel in plant nutrition. *Science* 280:918–21
53. Hisano T, Hata Y, Fujii T, Liu JQ, Kurihara T, et al. 1996. Crystal structure of L-2-haloacid dehalogenase from *Pseudomonas* sp. YL. An alpha/beta hydrolase structure that is different from the alpha/beta hydrolase fold. *J. Biol. Chem.* 271:20322–30
54. Houlne G, Boutry M. 1994. Identification of an *Arabidopsis thaliana* gene encoding a plasma membrane H^+-ATPase whose expression is restricted to anther tissue. *Plant J.* 5:311–17
55. Jahn T, Baluska F, Michalke W, Harper JF, Volkmann D. 1998. Plasma membrane H^+-ATPase in the root apex: evidence for strong expression in xylem parenchyma and asymmetric localization within cortical and epidermal cells. *Physiol. Plant.* 104:311–16
56. Jahn T, Fuglsang AT, Olsson A, Bruntrup IM, Collinge DB, et al. 1997. The 14-3-3 protein interacts directly with the C-terminal region of the plant plasma membrane H^+-ATPase. *Plant Cell* 9:1805–14
57. Johansson F, Sommarin M, Larsson C. 1993. Fusicoccin activates the plasma membrane H^+-ATPase by a mechanism involving the C-terminal inhibitory domain. *Plant Cell* 5:321–27
58. Jones DL, Shaff JE, Kochian LV. 1995. Role of calcium and other ions in directing root hair tip growth in *Limnobium stoloniferum* L. 1. Inhibition of tip growth by aluminium. *Planta* 197:672–80
59. Jorgensen PL, Andersen JP. 1988. Structural basis for E1-E2 conformational transitions in Na,K-pump and Ca-pump proteins. *J. Membr. Biol.* 103:95–120
60. Jorgensen PL, Nielsen JM, Rasmussen JH, Pedersen PA. 1998. Structure-function relationships of E1-E2 transitions and cation binding in Na,K-pump protein. *Biochim. Biophys. Acta* 1365:65–70
61. Jung KM, Kim DK. 2000. Purification and characterization of a membrane-associated 48-kilodalton phospholipase A_2 in leaves of broad bean. *Plant Physiol.* 123:1057–67
62. Kim DK, Lee HJ, Lee Y. 1994. Detection of two phospholipase A_2(PLA2) activities in leaves of higher plant *Vicia faba* and comparison with mammalian PLA2′s. *FEBS Lett.* 343:213–18
63. Kinoshita T, Shimazaki K. 1999. Blue light activates the plasma membrane H^+-ATPase by phosphorylation of the C terminus in stomatal guard cells. *EMBO J.* 18:5548–58

64. Korthout HAAJ, de Boer AH. 1994. A fusicoccin-binding protein belongs to the family of 14-3-3 brain protein homologs. *Plant Cell* 6:1681–92
65. Kraulis PJ. 1991. MOLSCRIPT—a program to produce both detailed and schematic plots of protein structures. *J. Appl. Crystallogr.* 24:946–50
66. Krysan PJ, Young JC, Sussman MR. 1999. T-DNA as an insertional mutagen in Arabidopsis. *Plant Cell* 11:2283–90
67. Krysan PJ, Young JC, Tax F, Sussman MR. 1996. Identification of transferred DNA insertions within Arabidopsis genes involved in signal transduction and ion transport. *Proc. Natl. Acad. Sci. USA* 93:8145–50
67a. Kühlbrandt W. 2000. Bacteriorhodopsin—the movie. *Nature* 406:569–70
68. Kühn C, Franceschi VR, Schulz A, Lemoine R, Frommer WB. 1997. Macromolecular trafficking indicated by localization and turnover of sucrose transporters in enucleate sieve elements. *Science* 275:1298–300
69. Lanfermeijer FC, Prins HBA. 1994. Modulation of H^+-ATPase activity by fusicoccin in plasma–membrane vesicles from oat (*Avena sativa* L.) roots—a comparison of modulation by fusicocin, trypsin, and lysophosphatiylcholine. *Plant Physiol.* 104:1277–85
70. Li YF, Hata Y, Fujii T, Hisano T, Nishihara M, et al. 1998. Crystal structures of reaction intermediates of L-2-haloacid dehalogenase and implications for the reaction mechanism. *J. Biol. Chem.* 273:15035–44
71. Lino B, Baizabal-Aguirre VM, Gonzalez de la Vara LE. 1998. The plasma-membrane H^+-ATPase from beet root is inhibited by a calcium-dependent phosphorylation. *Planta* 204:352–59
72. Luo H, Morsomme P, Boutry M. 1999. The two major types of plant plasma membrane H^+-ATPases show different enzymatic properties and confer differential pH sensitivity of yeast growth. *Plant Physiol.* 119:627–34
73. Lutsenko S, Kaplan JH. 1995. Organization of P-type ATPases: significance of structural diversity. *Biochemistry* 34:15607–13
74. MacLennan DH, Rice WJ, Green NM. 1997. The mechanism of Ca^{2+} transport by sarco(endo)plasmic reticulum Ca^{2+}-ATPases. *J. Biol. Chem.* 272:28815–18
75. Marra M, Fullone MR, Fogliano V, Masi S, Mattei M, et al. 1994. The 30 kilodalton protein present in purified fusicoccin receptor preparations is a 14-3-3-like protein. *Plant Physiol.* 106:1497–501
76. Maudoux O, Batoko H, Oecking C, Gevaert K, Vandekerckhove J, et al. 2000. A plant plasma membrane H^+-ATPase expressed in yeast is activated by phosphorylation at its penultimate residue and binding of 14-3-3 regulatory proteins in the absence of fusicoccin. *J. Biol. Chem.* 275:17762–70
77. Messerli M, Robinson KR. 1997. Tip localized Ca^{2+} pulses are coincident with peak pulsatile growth rates in pollen tubes of *Lilium longiflorum*. *J. Cell Sci.* 110:1269–78
78. Michel H. 1998. The mechanism of proton pumping by cytochrome c oxidase. *Proc. Natl. Acad. Sci. USA* 95:12819–24
79. Michelet B, Boutry M. 1995. The plasma membrane H^+-ATPase—a highly regulated enzyme with multiple physiological functions. *Plant Physiol.* 108:1–6
79a. Michelet B, Lukaszewicz M, Dupriez V, Boutry M. 1994. A plant plasma membrane proton-ATPase gene is regulated by development and environment and shows signs of a translational regulation. *Plant Cell* 6:1375–89
80. Moller JV, Juul B, le Maire M. 1996. Structural organization, ion transport, and energy transduction of P-type ATPases. *Biochim. Biophys. Acta* 1286:1–51

81. Moriau L, Michelet B, Bogaerts P, Lambert L, Michel A, et al. 1999. Expression analysis of two gene subfamilies encoding the plasma membrane H^+-ATPase in *Nicotiana plumbaginifolia* reveals the major transport functions of this enzyme. *Plant J.* 19:31–41
82. Morsomme P, Boutry M. 2000. The plant plasma membrane H^+-ATPase: structure, function and regulation. *Biochim. Biophys. Acta* 1465:1–16
83. Morsomme P, Dambly S, Maudoux O, Boutry M. 1998. Single point mutations distributed in 10 soluble and membrane regions of the *Nicotiana plumbaginifolia* plasma membrane PMA2 H^+-ATPase activate the enzyme and modify the structure of the C-terminal region. *J. Biol. Chem.* 273:34837–42
84. Morsomme P, de Kerchove d'Exaerde A, De Meester S, Thines D, Goffeau A, Boutry M. 1996. Single point mutations in various domains of a plant plasma membrane H^+-ATPase expressed in *Saccharomyces cerevisiae* increase H^+-pumping and permit yeast growth at low pH. *EMBO J.* 15:5513–26
85. Muslin AJ, Tanner JW, Allen PM, Shaw AS. 1996. Interaction of 14-3-3 with signaling proteins is mediated by the recognition of phosphoserine. *Cell* 84:889–97
86. Nakajima N, Saji H, Aono M, Kondo N. 1995. Isolation of cDNA for a plasma membrane H^+-ATPase from guard cells of *Vicia faba*. *Plant Cell Physiol.* 36:919–24
87. Obermeyer G, Lutzelschwab M, Heumann HG, Weisenseel MN. 1992. Immunolocalization of H^+-ATPases in the plasma-membrane of pollen grains and pollen tubes of *Lilium longiflorum*. *Protoplasma* 171:55–63
88. Oecking C, Eckerskorn C, Weiler EW. 1994. The fusicoccin receptor of plants is a member of the 14-3-3 superfamily of eukaryotic regulatory proteins. *FEBS Lett.* 352:163–66
89. Oecking C, Hagemann K. 1999. Association of 14-3-3 proteins with the C-terminal antoinhibitory domain of the plant plasma-membrane H^+-ATPase generates a fusicoccin-binding complex. *Planta* 207:480–82
90. Oecking C, Piotrowski M, Hagemeier J, Hagemann K. 1997. Topology and target interaction of the fusicoccin-binding 14-3-3 homologs of *Commelina communis*. *Plant J.* 12:441–53
91. Ogawa H, Haga T, Toyoshima C. 2000. Soluble P-type ATPase from an archaeon, *Methanococcus jannaschii*. *FEBS Lett.* 471:99–102
92. Olivari C, Pugliarello MC, Rasi-Caldogno F, De Michelis MI. 1993. Characteristics and regulatory properties of the H^+-ATPase in a plasma-membrane fraction purified from *Arabidopsis thaliana*. *Bot. Acta* 106:13–19
93. Olsson A, Svennelid F, Ek B, Sommarin M, Larsson C. 1998. A phosphothreonine residue at the C-terminal end of the plasma membrane H^+-ATPase is protected by fusicoccin-induced 14-3-3 binding. *Plant Physiol.* 118:551–55
94. Oufattole M, Arango M, Boutry M. 2000. Identification and expression of three new *Nicotiana plumbaginifolia* genes which encode isoforms of a plasma-membrane H^+-ATPase, and one of which is induced by mechanical stress. *Planta* 10:715–22
95. Palmgren MG. 1991. Regulation of plasma membrane H^+-ATPase activity. *Physiol. Plant.* 83:314–23
96. Palmgren MG. 1998. Proton gradients and plant growth: Role of the plasma membrane H^+-ATPase. *Adv. Bot. Res.* 28:1–70
97. Palmgren MG, Christensen G. 1994. Functional comparisons between plant plasma membrane H^+-ATPase isoforms expressed in yeast. *J. Biol. Chem.* 269:3027–33
98. Palmgren MG, Larsson C, Sommarin M. 1990. Proteolytic activation of the plant plasma membrane H^+-ATPase by removal of a terminal segment. *J. Biol. Chem.* 265:13423–26

99. Palmgren MG, Sommarin M, Serrano R, Larsson C. 1991. Identification of an autoinhibitory domain in the C-terminal region of the plant plasma membrane H^+-ATPase. *J. Biol. Chem.* 267:20470–75
100. Palmgren MG, Sommarin M, Ulvskov P, Jørgensen PL. 1988. Modulation of plasma membrane H^+-ATPase by lysophosphatidylcholine, free fatty acids and phospholipase A_2. *Physiol. Plant.* 74:11–19
101. Pardo JM, Serrano R. 1989. Structure of a plasma membrane H^+-ATPase gene from the plant *Arabidopsis thaliana*. *J. Biol. Chem.* 264:8557–62
102. Pardo JP, Slayman CW. 1988. The fluorescein isothiocyanate-binding site of the plasma-membrane H^+-ATPase of *Neurospora crassa*. *J. Biol. Chem.* 263:18664–68
103. Parets-Soler A, Pardo JM, Serrano R. 1990. Immunocytolocalization of plasma membrane H^+-ATPase. *Plant Physiol.* 93:1654–58
104. Parton RM, Fischer S, Malho R, Papasouliotis O, Jelitto TC, et al. 1997. Pronounced cytoplasmic pH gradients are not required for tip growth in plant and fungal cells. *J. Cell Sci.* 110:1187–98
105. Pedchenko VK, Nasirova GF, Palladina TA. 1990. Lysophosphatidylcholine specifically stimulates plasma membrane H^+-ATPase from corn roots. *FEBS Lett.* 275:205–8
106. Pedersen PL, Carafoli E. 1987. Ion motive ATPases. I. Ubiquity, properties and significance to cell function. *Trends Biochem. Sci.* 12:146–50
106a. Pedersen PA, Jorgensen JR, Jorgensen PL. 2000. Importance of conserved α-subunit segment ^{709}GDGVND for Mg^{2+} binding, phosphorylation, and energy transduction in Na,K-ATPase. *J. Biol. Chem.* 275:37588–95
107. Peitsch MC. 1996. ProMod and Swiss-Model: internet-based tools for automated comparative protein modelling. *Biochem. Soc. Trans.* 24:274–79
108. Piotrowski M, Morsomme P, Boutry M. 1998. Complementation of the *Saccharomyces cerevisiae* plasma membrane H^+-ATPase by a plant H^+-ATPase generates a highly abundant fusicoccin binding site. *J. Biol. Chem.* 273:30018–23
109. Portillo F. 2000. Regulation of plasma membrane H^+-ATPase in fungi and plants. *Biochim. Biophys. Acta* 1469:31–42
110. Post RL, Hegyvary C, Kume S. 1972. Activation by adenosine triphosphate in the phosphorylation kinetics of sodium and potassium ion transport adenosine triphosphatase. *J. Biol. Chem.* 247:6530–40
111. Rasi-Caldogno F, Pugliarello MC, Olivari C, De Michelis MI. 1993. Controlled proteolysis mimics the effect of fusicoccin on the plasma membrane H^+-ATPase. *Plant Physiol.* 103:391–98
112. Regenberg B, Villalba JM, Lanfermeijer FC, Palmgren MG. 1995. C-terminal deletion analysis of plant plasma membrane H^+-ATPase: yeast as a model system for solute transport across the plant plasma membrane. *Plant Cell* 7:1655–66
113. Rice WJ, MacLennan DH. 1996. Scanning mutagenesis reveals a similar pattern of mutation sensitivity in transmembrane sequences M4, M5, and M6, but not in M8, of the Ca^{2+}-ATPase of sarcoplasmic reticulum (SERCA1a). *J. Biol. Chem.* 271:31412–19
114. Ridder IS, Dijkstra BW. 1999. Identification of the Mg^{2+}-binding site in the P-type ATPase and phosphatase members of the HAD (haloacid dehalogenase) superfamily by structural similarity to the response regulator protein CheY. *Biochem. J.* 339:223–26
115. Ridder IS, Rozeboom HJ, Kalk KH, Dijkstra BW. 1999. Crystal structures of intermediates in the dehalogenation of

haloalkanoates by L-2-haloacid dehalogenase. *J. Biol. Chem.* 274:30672–78

116. Roelfsema MRG, Staal M, Prins HBA. 1998. Blue light-induced apoplastic acidification of *Arabidopsis thaliana* guard cells: Inhibition by ABA is mediated through protein phosphatases. *Physiol. Plant.* 103:466–74

116a. Rosenquist M, Sehnke P, Ferl RJ, Sommarin M, Larsson C. 2000. Evolution of the 14-3-3 protein family: Does the large number of isoforms in multicellular organisms reflect functional specificity? *J. Mol. Evol.* 51:446–58

117. Roussel A, Cambillau C. 1992. TURBO-FRODO, Biographics and AFMB (architecture et fonction des macromolécules biologiques), Marseilles, France

118. Sacchi GA, Cocucci M. 1992. Effects of deuterium oxide on growth, proton extrusion, potassium influx and *in vitro* plasma membrane activities in maize root segments. *Plant Physiol.* 100:1962–67

119. Samuels AL, Fernando M, Glass ADM. 1992. Immunofluorescent localization of plasma membrane H^+-ATPase in barley roots and effects of K nutrition. *Plant Physiol.* 99:1509–14

119a. Sayle R. 1996. RasMol Version 2.6 Molecular Visualization Program, Glaxo Wellcome Research Development, Stevenage, United Kingdom

120. Schaller GE, Sussman MR. 1988. Phosphorylation of the plasma-membrane H^+-ATPase of oat roots by a calcium-stimulated protein kinase. *Planta* 173:509–18

121. Scherer GF. 1994. Phospholipid signalling by phospholipase A_2 in plants. The role of mastoparan and lysophospholipids as weak 'auxin-like' agonists. *Symp. Soc. Exp. Biol.* 48:229–42

122. Schroeder JI. 1988. K^+ transport properties of K^+ channels in the plasma membrane of *Vicia faba* guard cells. *J. Gen. Physiol.* 92:667–83

123. Serrano R. 1989. Structure and function of plasma membrane ATPase. *Annu. Rev. Plant Physiol. Plant Mol. Biol.* 40:61–94

124. Seto-Young D, Hall MJ, Na S, Haber JE, Perlin DS. 1996. Genetic probing of the first and second transmembrane helices of the plasma membrane H^+-ATPase from *Saccharomyces cerevisiae*. *J. Biol. Chem.* 271:581–87

125. Slayman CL, Sanders D. 1985. Steady-state kinetic analysis of an electroenzyme. *Biochem. Soc. Symp.* 50:11–29

126. Sorensen TL, Dupont Y, Vilsen B, Andersen JP. 2000. Fast kinetic analysis of conformational changes in mutants of the Ca^{2+}-ATPase of sarcoplasmic reticulum. *J. Biol. Chem.* 275:5400–8

127. Soulimane T, Buse G, Bourenkov GP, Bartunik HD, Huber R, Than ME. 2000. Structure and mechanism of the aberrant ba_3-cytochrome c oxidase from *Thermus thermophilus*. *EMBO J.* 19:1766–76

128. Stadler R, Brandner J, Schulz A, 1995. Phloem loading by the *PmSUC2* sucrose carrier from *Plantago major* occurs into companion cells. *Plant Cell* 7:1545–54

129. Stadler R. Sauer N. 1996. The *Arabidopsis thaliana AtSUC2* gene is specifically expressed in companion cells. *Bot. Acta* 109:299–306

130. Stokes DL, Green NM. 2000. Modeling a dehalogenase fold into the 8-A density map for Ca^{2+}-ATPase defines a new domain structure. *Biophys. J.* 78:1765–76

131. Sussman MR. 1994. Molecular analysis of proteins in the plant plasma membrane. *Annu. Rev. Plant Physiol. Plant Mol. Biol.* 45:211–34

132. Svennelid F, Olsson A, Piotrowski M, Rosenquist M, Ottman C, et al. 1999. Phosphorylation of Thr-948 at the C terminus of the plasma membrane H^+-ATPase creates a binding site for the regulatory 14-3-3 protein. *Plant Cell* 11:2379–92

133. Sze H, Li X, Palmgren MG. 1999. Energization of plant cell membranes by H^+-pumping ATPases. Regulation and biosynthesis. *Plant Cell* 11:677–90

133a. The Arabidopsis Genome Initiative. 2000. Analysis of the genome sequence of the flowering plant *Arabidopsis thaliana*. *Nature* 408:796–815

134. Toyoshima C, Nakasako M, Nomura H, Ogawa H. 2000. Crystal structure of the calcium pump of sarcoplasmic reticulum at 2.6 Å resolution. *Nature* 405:647–55

135. Truernite E, Sauer N. 1995. The promoter of the *Arabidopsis thaliana SUC2* sucrose-H^+ symporter gene directs expression of beta-glucoronidase to the phloem—evidence for phloem loading and unloading by SUC2. *Planta* 196:564–70

136. Vara F, Serrano R. 1982. Partial purification and properties of the proton-translocating ATPase of plant plasma membranes. *J. Biol. Chem.* 257:12826–30

137. Vara F, Serrano R. 1983. Phosphorylated intermediate of the ATPase of plant plasma membranes. *J. Biol. Chem.* 258:5334–36

138. Vera-Estrella R, Barkla BJ, Higgins VJ, Blumwald E. 1994. Plant defence response to fungal pathogens—activation of host-plasma membrane H^+-ATPase by elicitor-induced enzyme dephosphorylation. *Plant Physiol.* 104:209–15

139. Villalba JM, Lützelschwab M, Serrano R. 1991. Immunocytolocalization of plasma-membrane H^+-ATPase in maize coleoptiles and enclosed leaves. *Planta* 185:458–61

140. Vilsen B, Andersen JP, Clarke DM, MacLennan DH. 1989. Functional consequences of proline mutations in the cytoplasmic and transmembrane sectors of the Ca^{2+}-ATPase of sarcoplasmic reticulum. *J. Biol. Chem.* 264:21024–30

141. Vilsen B, Andersen JP, MacLennan DH. 1991. Functional consequences of alterations to amino acids located in the hinge domain of the Ca^{2+}-ATPase of sarcoplasmic reticulum. *J. Biol. Chem.* 266:16157–64

142. Vilsen B, Andersen JP, MacLennan DH. 1991. Functional consequences of alterations to hydrophobic amino acids located at the M4S4 boundary of the Ca^{2+}-ATPase of sarcoplasmic reticulum. *J. Biol. Chem.* 266:18839–45

143. von Heijne G. 1992. Membrane protein structure prediction. Hydrophobicity analysis and the positive-inside rule. *J. Mol. Biol.* 225:487–94

144. Vonck J. 2000. Structure of the bacteriorhodopsin mutant F219L N intermediate revealed by electron crystallography. *EMBO J.* 19:2152–60

145. Wach A, Schlesser A, Goffeau A. 1992. An alignment of 17 deduced protein sequences from plant, fungi, and ciliate H^+-ATPase genes. *J. Bioenerg. Biomembr.* 24:309–17

146. Weisenseel MH, Dorn A, Jaffe LF. 1979. Natural H^+ currents traverse growing roots and root hairs of barley (*Hordeum vulgare* L.) *Plant Physiol.* 64:512–18

147. Weisenseel MH, Nuccitelli R, Jaffe LF. 1975. Large electrical currents traverse growing pollen tubes. *J. Cell Biol.* 66:556–67

148. Xing T, Higgins VJ, Blumwald E. 1996. Regulation of plant defense response to fungal pathogens: two types of protein kinases in the reversible phosphorylation of the host plasma membrane H^+-ATPase. *Plant Cell* 8:555–64

149. Yaffe MB, Rittinger K, Volinia S, Caron PR, Aitken A, et al. 1997. The structural basis for 14-3-3:phosphopeptide binding specificity. *Cell* 91:961–71

149a. Young JC, Krysan PJ, Sussman MR. 2001. Efficient screening of Arabidopsis T-DNA insertion lines using degenerate primers. *Plant Physiol.* 125:513–18

150. Zeiger E. 1983. The biology of stomatal guard cells. *Annu. Rev. Plant Physiol.* 34:441–75
151. Zhang Z, Sumbilla C, Lewis D, Summers S, Klein MG, Inesi G. 1995. Mutational analysis of the peptide segment linking phosphorylation and Ca^{2+}-binding domains in the sarcoplasmic reticulum Ca^{2+}-ATPase. *J. Biol. Chem.* 270:16283–90
152. Zhao R, Dielen V, Kinet JM, Boutry M. 2000. Cosuppression of a plasma membrane H^+-ATPase isoform impairs sucrose translocation, stomatal opening, plant growth, and male fertility. *Plant Cell* 12:535–46

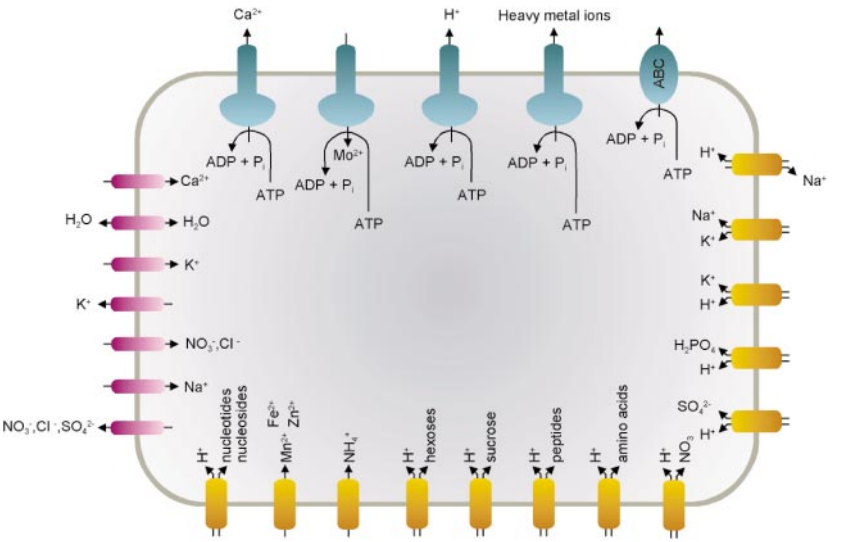

Figure 1 Overview of transport proteins in the plasma membrane of plant cells and their proposed transport specifities. Transport through most channel proteins (red) and carrier proteins (orange) is energized by the membrane potential (negative on the inside) and proton gradient generated by the plasma membrane H^+-ATPase (blue, middle).

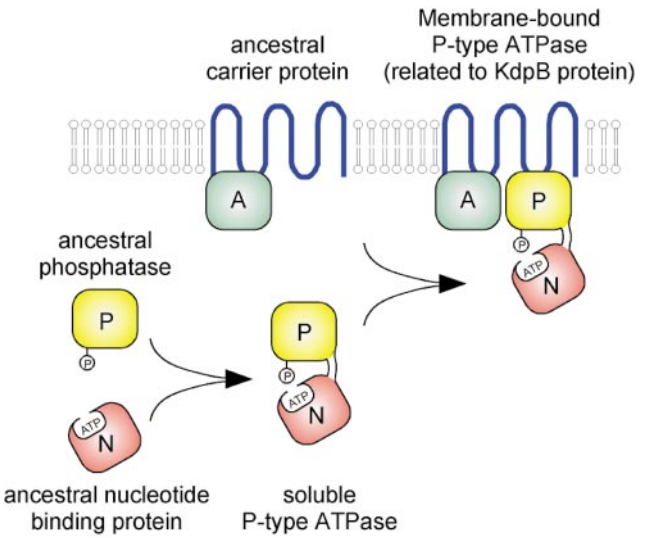

Figure 2 Proposed evolution of plasma membrane H^+-ATPases. Two soluble proteins, a protein phosphatase (*P*) and a nucleotide-binding protein (*N*), fused to form a soluble P-type ATPase. This later fused with a membrane-bound carrier protein with six trans-membrane spanning segments to form an ATP-fueled cation pump. As a result of additional fusion events, present day H^+-ATPases have ten trans-membrane segments.

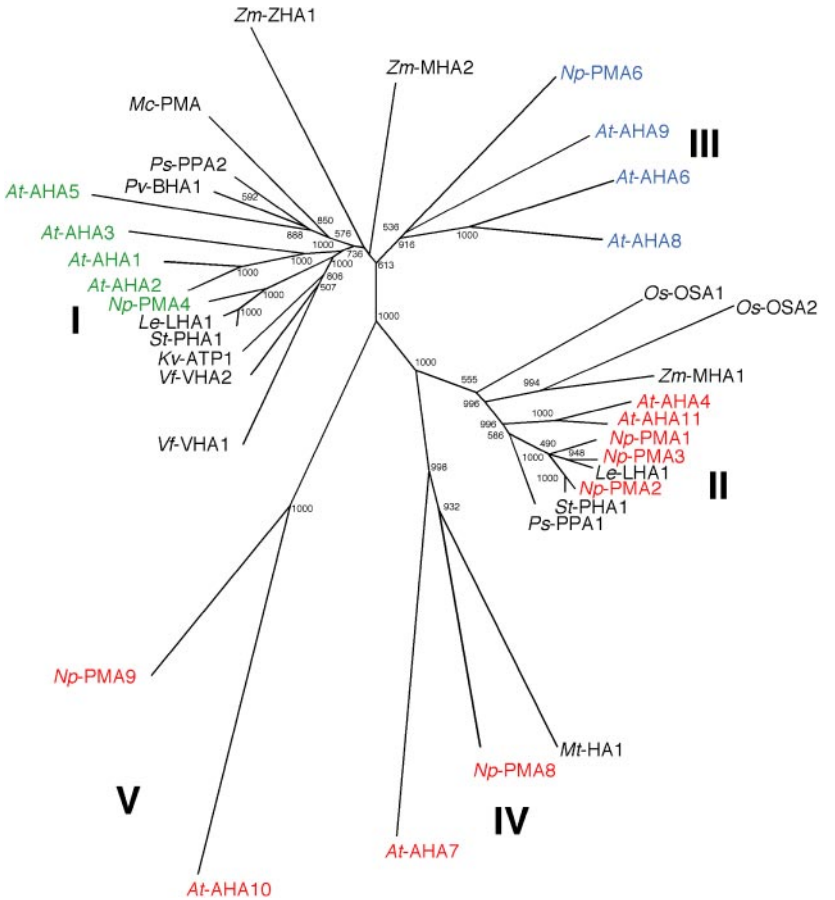

Figure 3 Phylogenetic tree showing the predicted relationship among plant plasma membrane H^+-ATPases. The PHYLIP program (J Felsenstein, University of Washington) was used to construct the phylogenetic tree from the amino acid sequences deduced from genomic and cDNA clones. Colors indicate H^+-ATPases that have a very similar exon structure (see Figure 4). Sequences are from *Arabidopsis thaliana* (AHA1: P20649; AHA2: P19456; AHA3: P20431; AHA4: Q9SU58; AHA5: Q9SJB3; AHA6: Q9SH76; AHA7: Q9LY32; AHA8: Q9M2A0; AHA9: Q42556; AHA10: Q43128; AHA11: Q9LV11), *Nicotiana plumbaginifolia* (PMA1: Q08435; PMA2: Q42932; PMA3: Q08436; PMA4: Q03194; PMA6: Q9SWH2; PMA8: Q9SWH1; PMA9: Q9SWH0), *Kosteletzkya virginica* (KvATP1: O22613), *Lycopersicon esculentum* (LHA1: P22180; LHA2: Q9SPD5; LHA4: Q96578), *Medicago truncatula* (ha1: Q9M4N4), *Mesembryanthemum crystallinum* (PMA: P93265), *Oryza sativa* (OSA1: Q43001; OSA2: Q43002), *Phaseolus vulgaris* (BHA1: Q43106), *Prunus persica* (PPA1: Q9M460; PPA2: Q9M461), *Solanum tuberosum* (PHA1: Q43182; PHA2: Q41378), *Vicia faba* (VHA1: Q43131; VHA2: Q9SAW3), *Zea mays* (MHA1: Q43243; MHA2: Q43271), *Zostera marina* (ZHA1: Q43275).

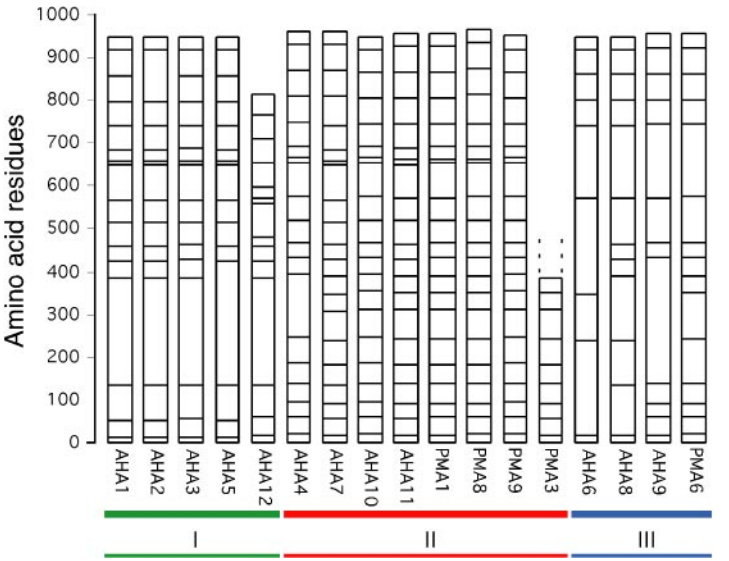

Figure 4 Schematic representation of the position of exon boundaries in the genomic sequences of Arabidopsis and *Nicotiana plumbaginifolia* H^+-ATPases. The positions of introns are shown by a horizontal line within a box representing the coding sequence.

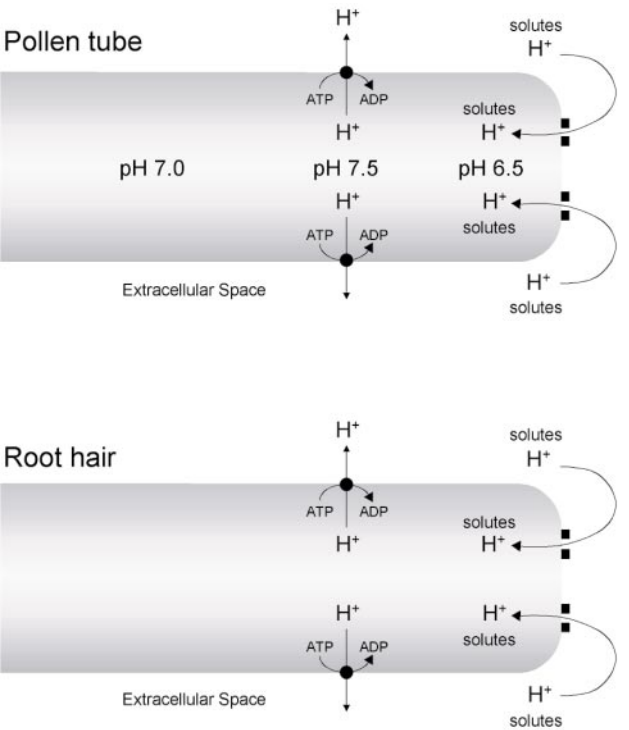

Figure 5 A model for proton gradients in pollen tubes and root hairs. Data related to pollen tubes are from Feijo et al (35).

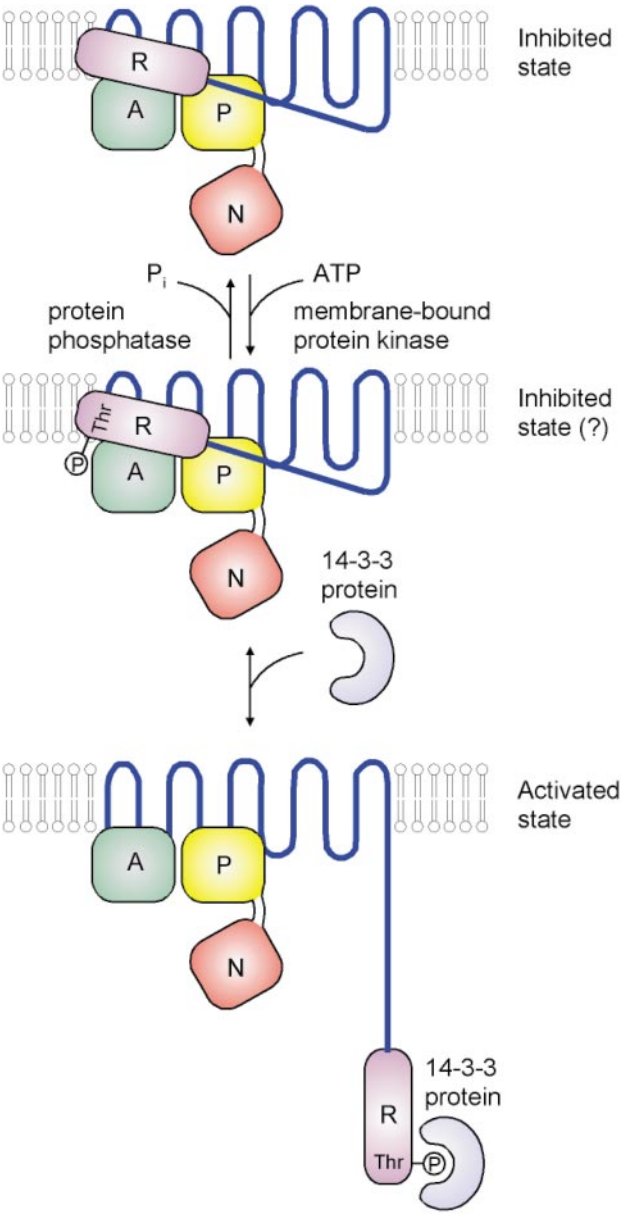

Figure 6 A model for posttranslational regulation of plasma membrane H^+-ATPase involving a protein kinase and protein phosphatase pair that has the R-domain as its target. Regulatory 14-3-3 protein recognizes a binding site generated by phosphorylation of the R-domain.

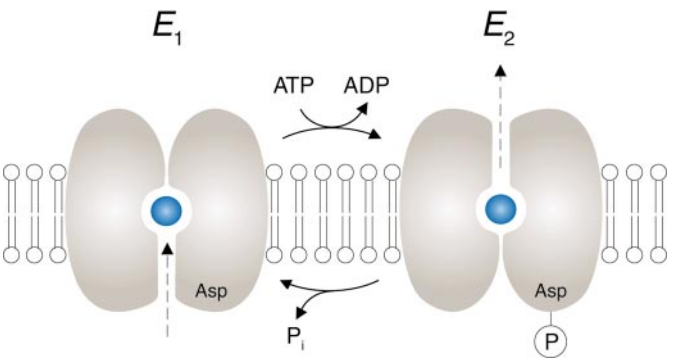

Figure 7 A model for the transport mechanism of plasma membrane H^+-ATPase. H^+ (or H_3O^+) binds to a specific ion binding pocket, the accessibility of which is alternating between the two sites of the membrane during the catalytic cycle. In the E_1 conformation, the ion binding pocket is accessible to the cytoplasmic side of the membrane only. In the E_2 conformation, the ion binding pocket is accessible to the extracellular side of the membrane. Differences in affinity of the ion binding site in the two conformations dictate whether the ion is bound or released.

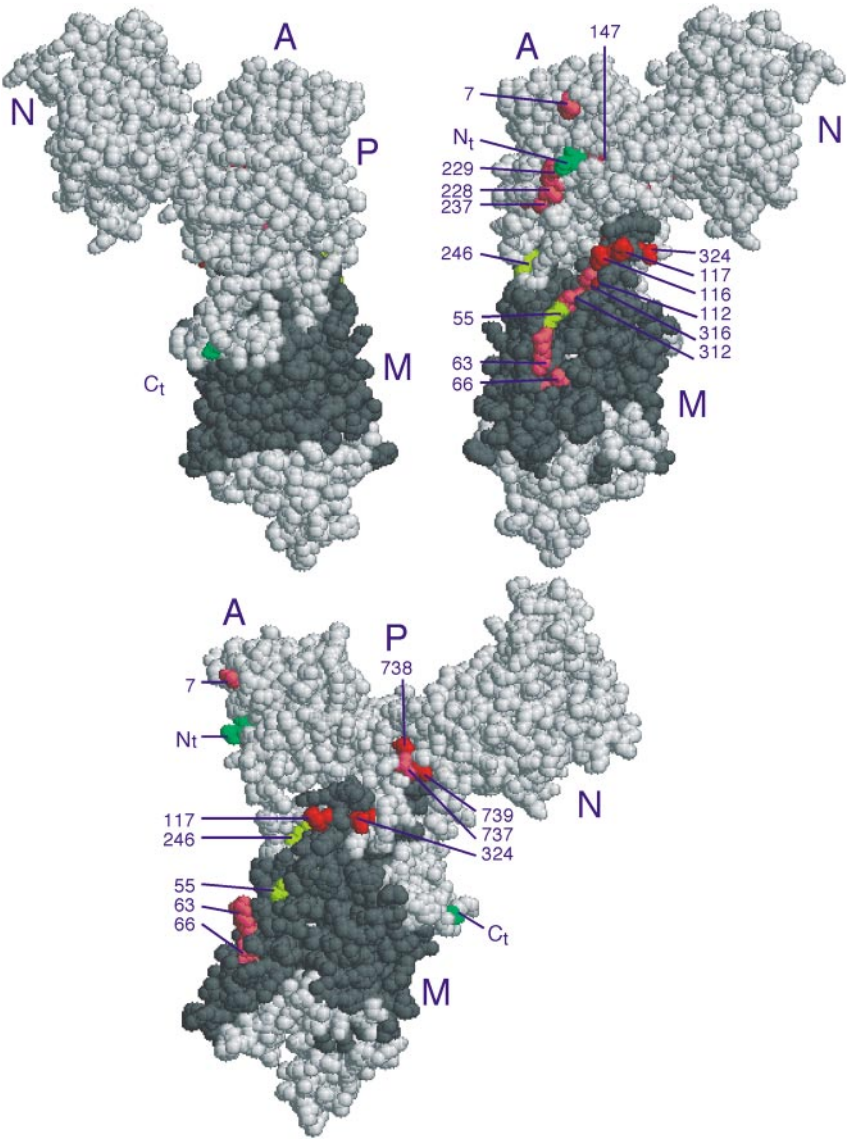

Figure 8 Space-filling model of the three-dimensional structure of sarcoplasmic reticulum Ca^{2+}-ATPase (PDB entry 1eul; 134). The corresponding residues that in a number of other P-type ATPases give rise to activation of pump activity when mutated are colored pink (*N. plumbaginifolia* PMA2 H^+-ATPase), red (*Saccharomyces cerevisiae* PMA1 H^+-ATPase), and yellow (*A. thaliana* ACA4 Ca^{2+}-ATPase). A complete list of these residues is presented in Table 4. Dark gray indicates membrane-spanning alpha-helices. The protein model was generated with the RasMol software program (22).

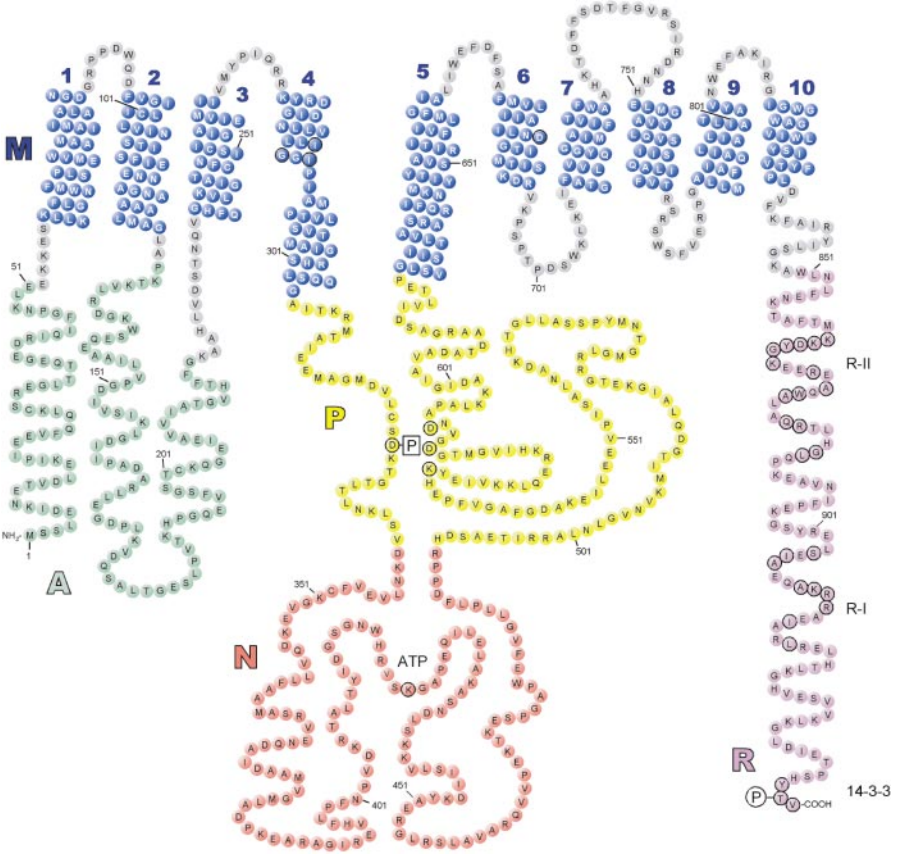

Figure 9 Schematic presentation of the AHA2 plasma membrane H^+-ATPase. The various domains (A, P, N, and R) of the enzyme are indicated by colored residues. Encircled residues are discussed further in the text. The positions of transmembrane segments M1-M7 are in accordance with the corresponding residues in the sarcoplasmic reticulum Ca^{2+}-ATPase (134). The predicted topologies of M8-M10 were analyzed by the method of von Heijne (143). R-I: Region I; R-II: Region-II; 14-3-3: 14-3-3 protein binding site.

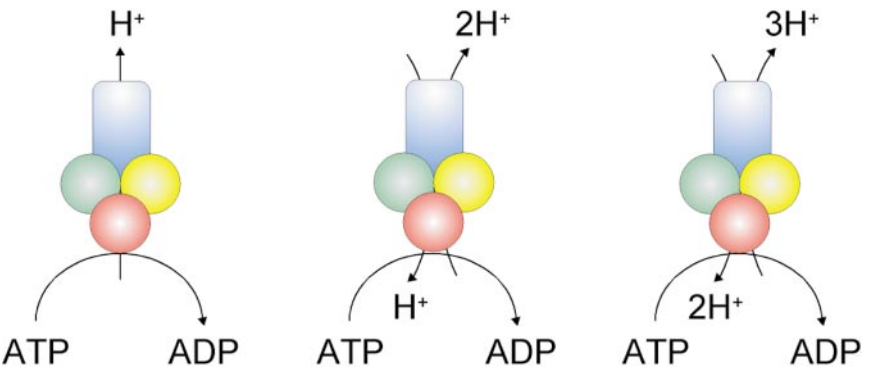

Figure 10 Models for proton pumping by plasma membrane H^+-ATPase that result in a 1:1 stoichiometry between ATP hydrolyzed and net proton transport.

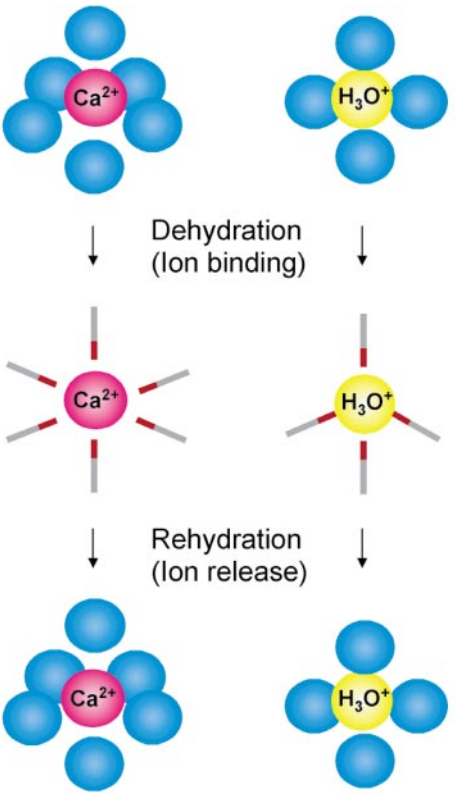

Figure 11 Proposed model for dehydration and rehydration of Ca^{2+} and H^{+} accompanying binding and release from the cation binding pockets in the Ca^{2+} and H^{+}-ATPases, respectively.

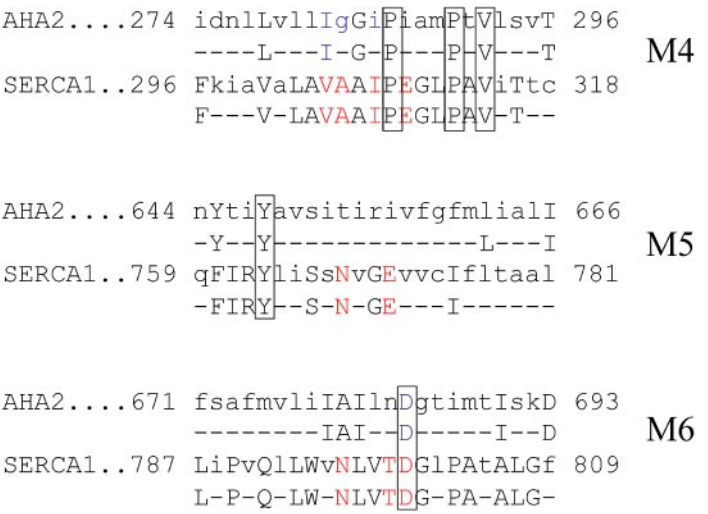

Figure 12 Alignment of selected trans-membrane segments of the AHA2 plasma membrane H^+-ATPase and the sarcoplasmic reticulum Ca^{2+}-ATPase SERCA1. Conserved residues in both pumps are boxed. Residues conserved in 30 out of 39 H^+-ATPase sequences and 46 out of 58 Ca^{2+}-ATPase sequences in the databases are indicated by capital letters. Residues involved in Ca^{2+} binding are colored red. Residues proposed to be involved in H^+ binding are colored blue.

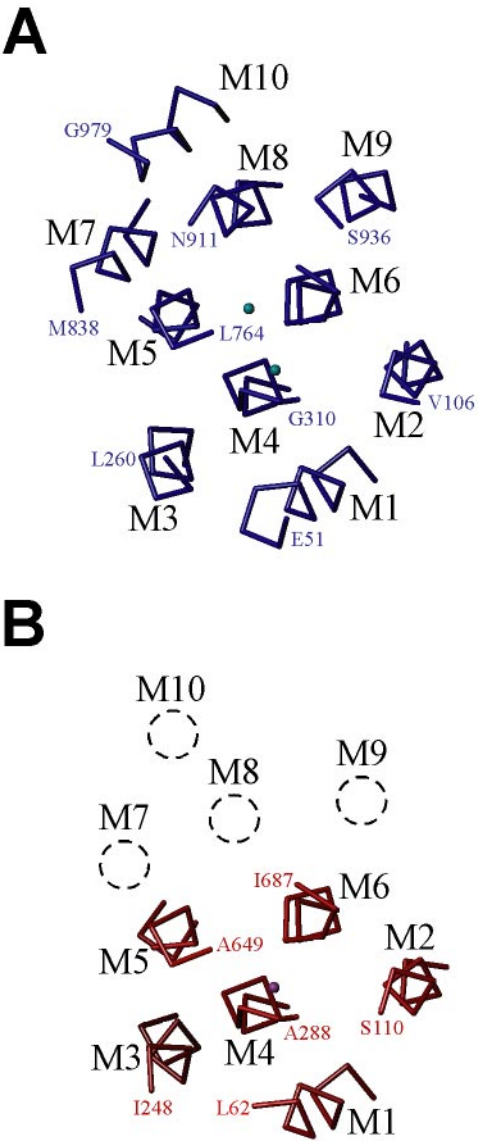

Figure 13 Top view of the transmembrane helices of the sarcoplasmic reticulum Ca^{2+}-ATPase SERCA1 (*A*) and in the model of AHA2 plasma membrane H^+-ATPase (*B*). The pictures were constructed (*A*) from the Protein Database (PDB) entry 1eul (134) or (*B*) from a homology model of AHA2 (J Bukrinsky, MJ Buch-Pedersen, S Larsen, MG Palmgren, submitted). Ten residues are shown from each of the helices shown. Dashed circles indicate transmembrane helices that could not be modeled. Green spheres, Ca^{2+}; red sphere, H_3O^+. The figure was generated using the program TURBO-FRODO (117).

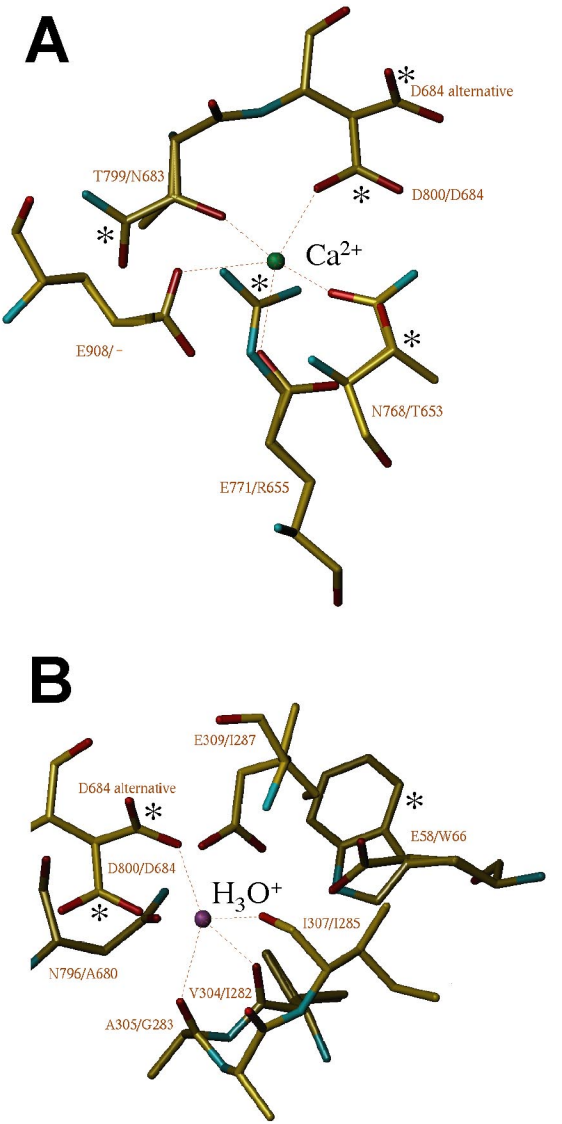

Figure 14 Cation binding sites I (*A*) and II (*B*) in the Ca^{2+}-ATPase SERCA1 (*upper label*) superimposed on the corresponding residues from the model of AHA2 (*lower label*, marked by asterisks). The model of AHA2 (J Bukrinsky, MJ Buch-Pedersen, S Larsen, MG Palmgren, submitted) is based on the structure of the sarcoplasmic reticulum Ca^{2+}-ATPase SERCA1 (PDB entry 1eul; 134). Green sphere, Ca^{2+}; red sphere: H_3O^+. The figure was generated using the program TURBO-FRODO (117).

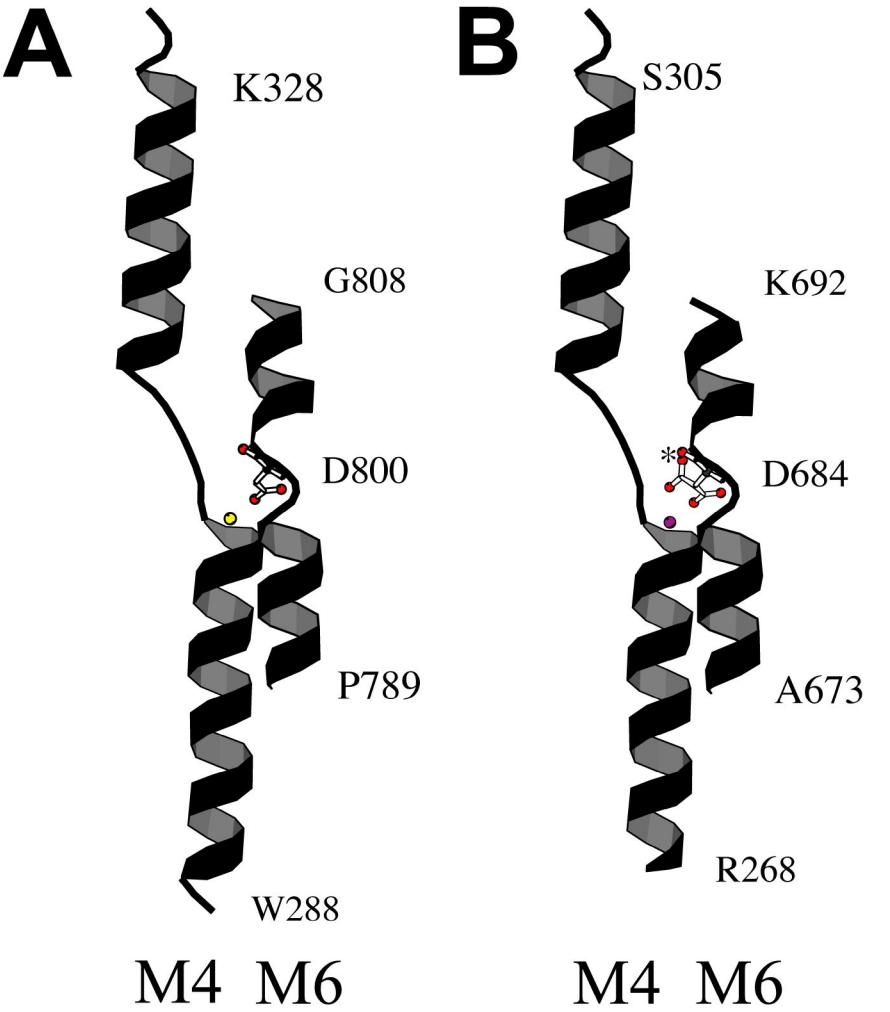

Figure 15 Transmembrane helices M4 and M6 in ribbon from the sarcoplasmic reticulum Ca^{2+}-ATPase SERCA1 (*A*) and a homology model of the AHA2 plasma membrane H^{+}-ATPase (*B*). (*A*) D800 in SERCA1 (PDB) entry 1eul (134), which is bridging the two Ca^{2+} ions bound, is shown in ball-and-stick. (*B*) The corresponding arrangement in the model of AHA2 (J Bukrinsky, MJ Buch-Pedersen, S Larsen, MG Palmgren, submitted), with D684 shown in two possible conformations (one of which is marked by an asterisk). Yellow sphere, Ca^{2+}; red sphere, H_3O^{+}. This figure was produced with the program MOLSCRIPT (65).

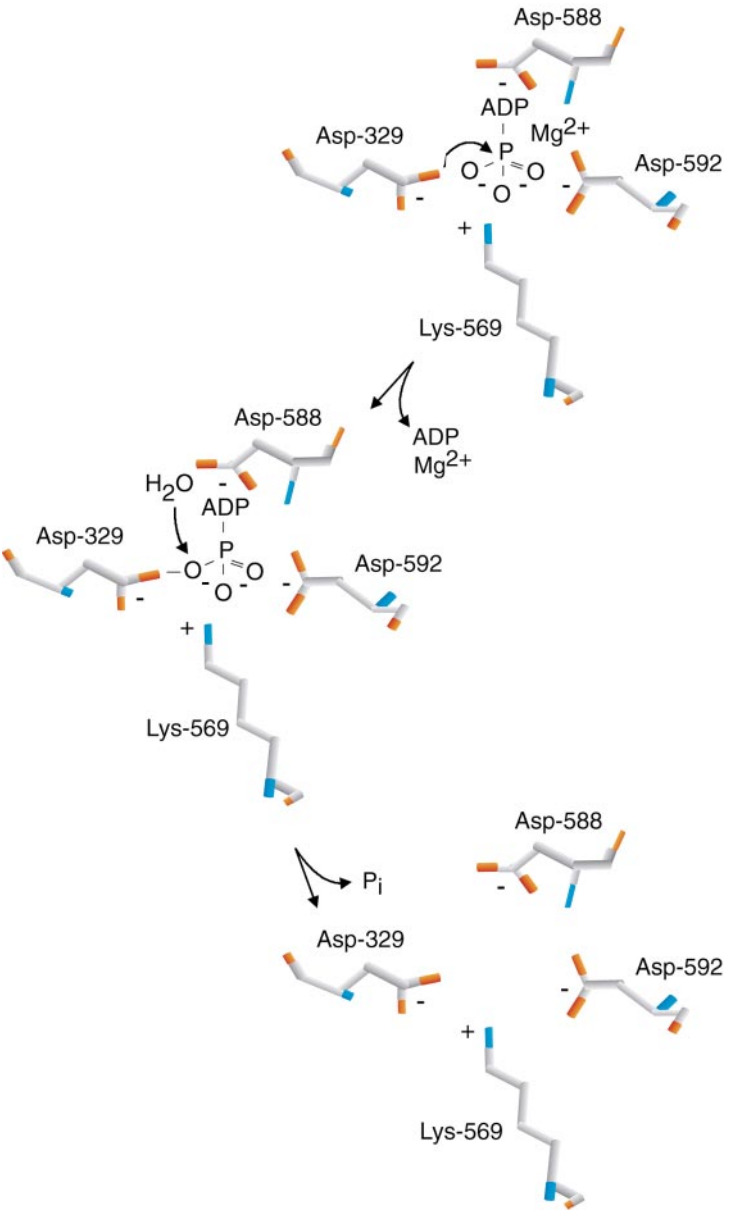

Figure 16 Proposed reaction scheme for the phosphorylation during catalysis of plasma membrane H^+-ATPases. For details see the text.

Annual Review of Plant Physiology and Plant Molecular Biology
Volume 52, 2001

CONTENTS